Proceedings of International Conference
Applications of Structural Fire Engineering
Prague, 19-20 February 2009

Session 8

Other Questions

SEISMIC AND FIRE DESIGN OF COMPOSITE FRAMES

A multi-disciplinary approach for an integrated design

Elisabetta Alderighi [a], Walter Salvatore [a]

[a] University of Pisa, Department of Civil Engineering, Pisa, Italy

INTRODUCTION

Seismic and fire design of a building structure may be two very demanding tasks especially if included in a performance-based design philosophy, so that a multidisciplinary approach is needed. For the time being, the harmonization on the regulations for these two design fields is almost missing; moreover, while performance-based approach to seismic design has widely developed in last years and introduced by many countries into standards and regulations, the same cannot be said for performance-based design of structures in fire whose application is still limited in scope.
In addition, while many studies have been done on risk assessment for daily fires, there have been very few works on risk assessment and damage evaluation of a building after an earthquake.
In present work, a comprehensive methodology for the evaluation of the structural fire performance of earthquake resistant frames including post-earthquake fire scenarios is presented and applied to a set of composite frames in order to identify an optimized solution with respect to all design actions. Seismic and fire are at first considered as independent hazards, this allowing for the identification of the key structural parameters governing each design phase and thus for their correlation.
Once seismic and fire design issues are met, post-earthquake fire scenarios are investigated showing that control of fires in a building after earthquakes can be possible if the buildings are designed with good earthquake resistance, good fire resistance rating and good overlap between the two.

1 THE PROPOSED PERFORMANCE-BASED DESIGN METHODOLOGY

Actual code provisions such as the Eurocodes develop seismic and fire design of structures according to completely independent tools, this preventing the possibility of obtaining an integrated design. It's only in the last years that adopting the idea developed in performance-based earthquake engineering some design procedures have been developed ([1], [2]) accounting for the integration of structural fire safety into the design of framing systems and analyzing buildings subjected to an earthquake and to the subsequent fire (see Figs. 1 and 2). However, even if the evaluation of the state of the structure after the earthquake was posed as a fundamental step, no indication was given of means of quantifying the seismic-induced damage. Moreover, no attention was paid to the necessary harmonization between seismic and fire design fields to promote an integrated design.

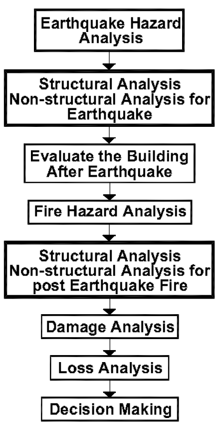

Fig. 1. Lee et al., 2004 [1]

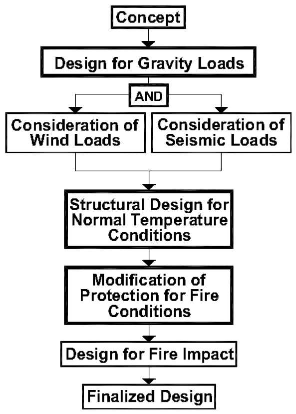

Fig. 2. Johann et al., 2006 [2]

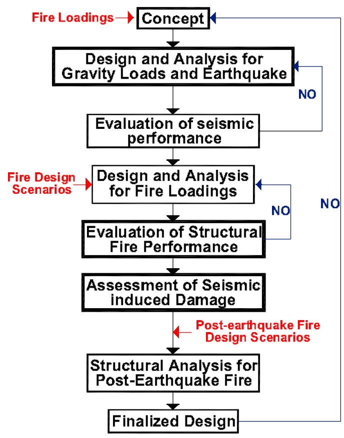

Fig. 3. Proposed methodology

In present paper, a comprehensive methodology for the assessment of the fire performance of earthquake resistant frames including post-earthquake fire design scenarios is presented (see Fig. 3). The starting point is represented by the conceptual design of the building structure meaning that all design issues are carefully evaluated and taken into account since the early design stages, this being very important in order to gather information on the effectiveness of different possible structural solutions. The obtained result is the definition of a set of composite frames to which the proposed methodology is applied in order to identify an optimized solution with respect to all design actions. Afterwards, the process is divided into two main macro-steps consisting in design and evaluation of the structural performance under seismic and fire loadings when these two are considered as independent hazards. In this way, the related design actions are applied in separate conditions and the resulting structural behaviour is carefully evaluated. The importance of separating these two design/performance evaluation phases consists in the identification of the most relevant structural parameters governing each design phase, in order to correlate them for the obtainment of an integrated design solution. In the last step, the post-earthquake fire performance of the frame is re-evaluated by taking into account suitably defined design scenarios.

2 THE COMPOSITE FRAMES: CONCEPTUAL DESIGN

In order to choose the most suitable structural solution with respect to all design actions, several frames with the same geometric layout, but different members typologies as defined in the framework of a Europeans Research Project [3] were investigated and summarized in Table 1.

Table 1. Analyzed structural solutions for beam and column elements

Frame Type	Main beams	Composite Columns
Type A1	IPE (bare steel)	HEB (partially encased)
Type A2	IPE (composite with ribbed steel sheeting)	HEB (partially encased)
Type B1	IPE (bare steel)	CHS (circular concrete filled)
Type B2	IPE (composite with ribbed steel sheeting)	CHS (circular concrete filled)

For each solution, the main frame was made out of two bays spanning 7,5 and 10 m, respectively while the secondary beams, spanning 7,5 m each, were placed at a distance of 2,5 m and were designed according to a simply supported scheme (see Fig.4) so that the frame resulted braced in transversal direction. For what concerns the elevation, a medium-rise solution was adopted including five floors with 3,5 m inter-storey height.
At this stage, a preliminary investigation on the load bearing capacity at elevated temperature of the two kinds of composite columns was developed and obtained results showed [4,5] that the concrete filled solution offered a more satisfactory behaviour in fire with respect to the partially encased one.

3 DESIGN AND PERFORMANCE FOR VERTICAL AND SEISMIC LOADINGS

In the first macro-step of the design procedure, gravity loads in the static combination of actions were applied and afterwards, seismic design was developed according to the lateral force method of analysis with reference to the so called “strong column – weak beam” concept. Seismic design actions were determined considering a behaviour factor $q = 6$, meaning high ductility class (HDC).
An extensive presentation of the obtained results is reported in previous works [4, 5, 6], anyway the main findings in terms of members’ sizing are summarized in Table 2.

Table 2. Members’ sizing according to different combinations of actions

	Static combination of actions (EC3 / EC4)		Seismic combination of actions (EC8)	
Frame	Main beam	Composite Column	Main beam	Composite Column
Type A1	IPE450 (bare steel)	HEB340	IPE450 (bare steel)	HEB450
Type A2	IPE400 (composite)	HEB340	IPE400 (composite)	HEB400
Type B1	IPE450 (bare steel)	CHS355/10	IPE450 (bare steel)	CHS508/14 (not commercial)
Type B2	IPE400 (composite)	CHS355/10	IPE400 (composite)	CHS457/12

It was observed that in the static combination the use of a composite section for the main beams did not allow for a substantial reduction of the steel joist with respect to the bare steel solution and this because the adoption of a moment resisting scheme do not allow taking advantage of the composite action in hogging bending regions, especially for long spans. Afterwards, when passing from static to seismic design, the size of beams' cross sections was unchanged meaning that their sizing is governed by the static combination of actions. Moreover, in the framework of the adopted linear elastic analysis, severe limitations were imposed on the selection of columns cross-sections, especially when coupled with bare steel beams (type A1, type B1) since the last do not add a significant contribution to the global lateral stiffness of the frame. This phenomenon was evident for type B1 frame where no commercial column cross-section with the required amount of flexural stiffness satisfying the serviceability limit states was available. Conversely, the combination with composite beams (type B2) allowed for smaller columns cross-sections, this limiting both frame self-weight and fundamental period.
Afterwards, the seismic performance of each structural solution was evaluated by means of static non linear analysis; obtained results [4, 5] showed that all the analyzed solutions offered a satisfactory behaviour under seismic actions.

4 DESIGN AND PERFORMANCE FOR FIRE LOADINGS

In the second macro-step of the procedure, the structural fire performance of the unprotected frames was evaluated by using the program SAFIR [7]. Considering that in seismic design the importance of the relative stiffness between beam and column elements was outlined, three situations accounting for different values of the flexural stiffness ratio r were investigated to assess its influence in fire situation, and thus setting a correlation between the two design fields.
In particular, the analyzed frames were Type B2 ($r \sim 1$) and Type A1 ($r < 1$) designed for the seismic combination of actions and Type B2 ($r > 1$) designed for the static combination of actions.
Tracing an analogy with performance-based seismic design, a stiffness hierarchy criterion was defined being the condition $r > 1$, identified as "soft columns – stiff beams" and the condition $r < 1$ identified as "stiff columns – soft beams".
Thermo – mechanical analyses were performed with reference to the same fire design scenario considering fire applied to beam and column elements at the second floor level; the obtained results were expressed in terms of evolution of the axial force in the longest span beam, this being the most representative curve of the global frame behaviour in fire, as shown in Fig. 5.

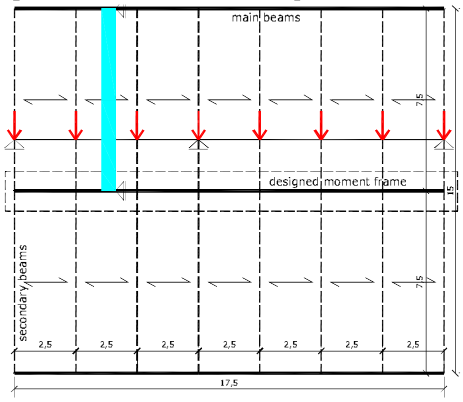

Fig. 4. Typical floor layout

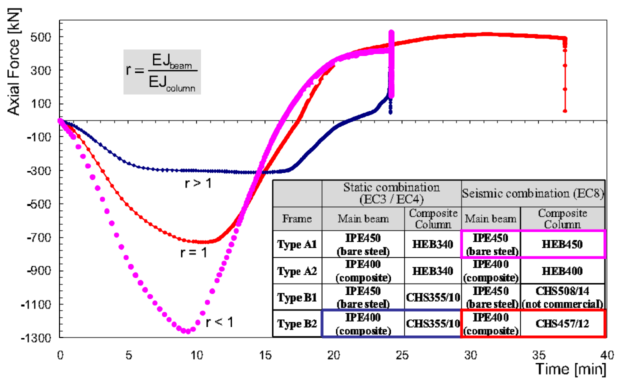

	Static combination (EC3 / EC4)		Seismic combination (EC8)	
Frame	Main beam	Composite Column	Main beam	Composite Column
Type A1	IPE450 (bare steel)	HEB340	IPE450 (bare steel)	HEB450
Type A2	IPE400 (composite)	HEB340	IPE400 (composite)	HEB400
Type B1	IPE450 (bare steel)	CHS355/10	IPE450 (bare steel)	CHS508/14 (not commercial)
Type B2	IPE400 (composite)	CHS355/10	IPE400 (composite)	CHS457/12

Fig. 5. Axial force in the heated beams

It was observed that the frames designed with $r > 1$ and $r < 1$, possess a quite lower global fire resistance rating than the frame with $r \sim 1$; besides, the obtained curves have quite different shapes. The "static" Type B2 frame ($r > 1$) was not able to able to develop catenary action since the column elements, being too flexible, were not able to provide a sufficient axial restraint to the heated beam; moreover, the compressive peak was replaced by a constant field characterized by a low intensity.

Conversely, the behaviour of the “seismic” Type A1 frame (r < 1) was characterized by a sharp compressive peak and a reduced duration of the developed catenary action; in this case, because of the high flexural stiffness of column elements high values of the axial compressive force are induced in the heated beam, this causing its premature failure. The adopted numerical model wasn’t able to catch local buckling phenomena, but it’s clear that having high values of compressive force in the beam can induce early local buckling of the compressed steel flanges at supports, especially for earthquake resistant frames where the continuity of joints increases such phenomenon [4].
Finally, the performed analysis showed that the “seismic” Type B2 frame (r ~1) offer the best performance with respect to both seismic and fire actions when these are considered as independent hazards, since it offered near 40 minutes of fire resistance rating even if unprotected [8].
Therefore, such a solution was chosen as reference study case and thermo – mechanical analyses in the post-earthquake fire situation were developed, as reported in the next section.
In present work, no account is taken of the earthquake induced structural damage, anyway extensive details and results on the matter may be found in [9].

5 POST-EARTHQUAKE STRUCTURAL FIRE PERFORMANCE

When considering post-earthquake fire situations, different design scenarios have to be taken into account; this would require a comprehensive post-earthquake fire risk assessment involving both analysis and prediction of fire spreading inside the building.
This work focused on structural issues only and some earthquake “indirect” effects were taken into account in a simplified way, namely: the debonding of the steel sheeting from the concrete slab and the possibility of fire spreading between two adjacent compartments.
In each case, the fire performance of the “damaged” frame was evaluated in terms of its global fire resistance rating and compared with the performance in “undamaged” conditions.

5.1 Debonding of the steel sheeting from the concrete slab

The cyclic action of earthquake loadings may induce a debonding effect of the steel sheeting from the concrete slab; for this reason, considering the presence of the steel sheeting in a post-earthquake fire situation could not represent a safe-sided choice.
In present work, the fire resistance rating of the frame is re-evaluated neglecting the presence of the steel sheeting in order to assess its influence on the global frame structural fire behaviour.

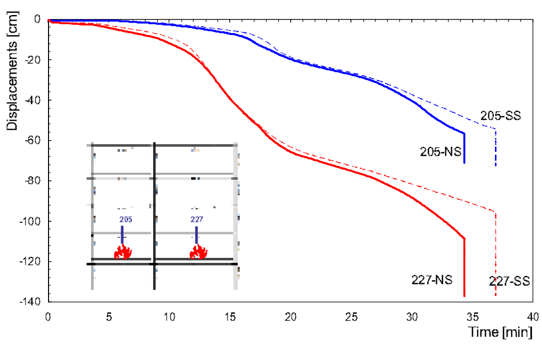

Fig. 6. Vertical displacements at mid-span

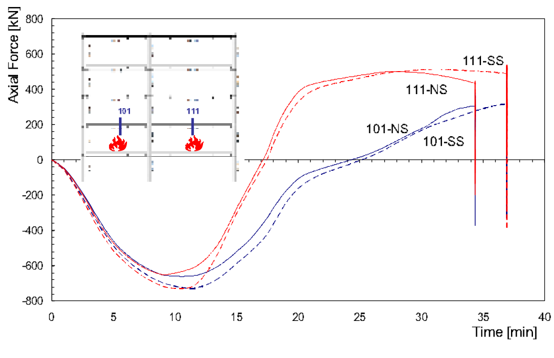

Fig. 7. Axial force in the heated beams

The evolution of vertical displacements at mid-span of heated beams is shown in Fig. 6. When neglecting the steel sheeting (NS), the beams undergo higher displacements at mid-span, especially in the catenary action regime, the steel sheeting offering additional tensile strength and stiffness to the composite beam when loads are carried in tension. It’s worth to notice that the contribution of the steel sheeting is relevant mainly in the later stages of fire this being in contrast with standard design practice where because of elevated temperatures the sheeting is supposed to have lost its strength and its contribution is neglected.

The evolution of internal actions was checked as well; with particular attention to the evolution of axial force, as shown in Fig. 7. In this case, neglecting the steel sheeting caused a reduction of the peak compressive force due to the limited expansion of the beam in the heating phase, this inducing a lower restraining force offered by column elements.
Comparing the global fire resistance rating in the two situations, it was shown that the presence of steel sheeting can partly enhance the structural fire behaviour by adding a 7% to the surviving time. Moreover, the Code assumption of considering the steel sheeting bonded to the concrete slab for all the duration of the fire is revealed to be not on the safe side in a post-earthquake fire situation.

5.2 Simultaneous fire spreading in two adjacent compartments

The loss of separating function normally covered by the slab due to extensive seismic-induced concrete cracking may be considered a realistic post-earthquake fire situation increasing the possibility of fire spreading between two adjacent compartments.
In present analysis, it is supposed that a fire can simultaneously start at the first (F1) and second (F2) floor levels, these representing the "weakest" parts of the frame at an earthquake as showed by the distribution of plastic hinges obtained by non-linear static analysis [4, 6].

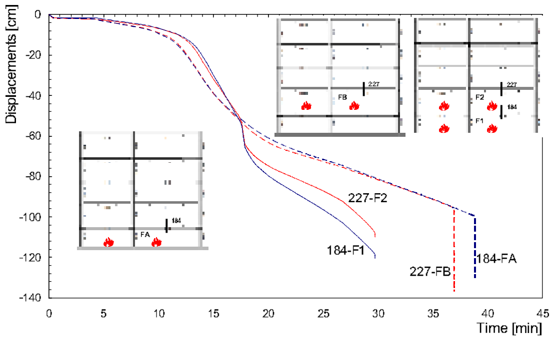

Fig. 8. Vertical displacements at mid-span

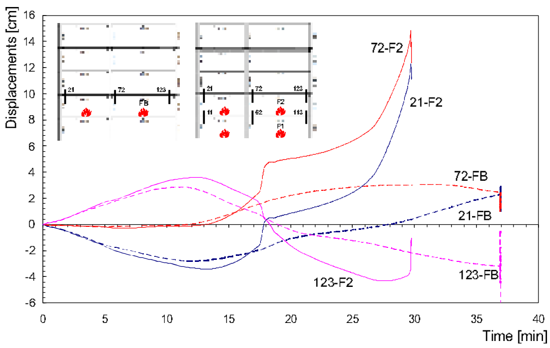

Fig. 9. Horizontal displacements at supports

The evolution of displacements and the distribution of stresses at critical cross-section for the longest span beam were deeply investigated; obtained results were compared with two "undamaged" situations: FA - fire at first floor level only and FB - fire at second floor level only.
The evolution of vertical displacements at mid-span is shown in Fig. 8; the picture shows the tendency of the beams F1 and F2 to move into run-away deflections once the catenary action begins. This is prevented by column elements allowing for higher vertical displacements if compared with the beams FA and FB. For the same reason, vertical displacements are lower in the early stages since beam elements are allowed higher expansion and there is less need to accommodate the restrained thermal elongation through bowing deflections.

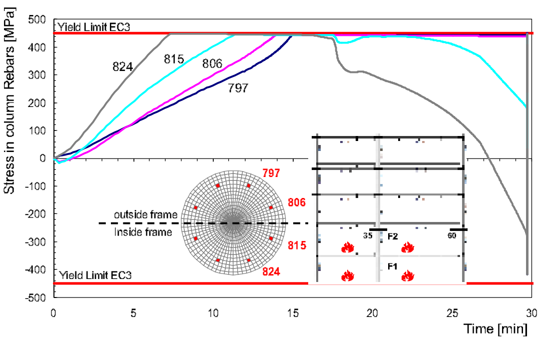

Fig. 10. Top interior column (35): re-bars stress

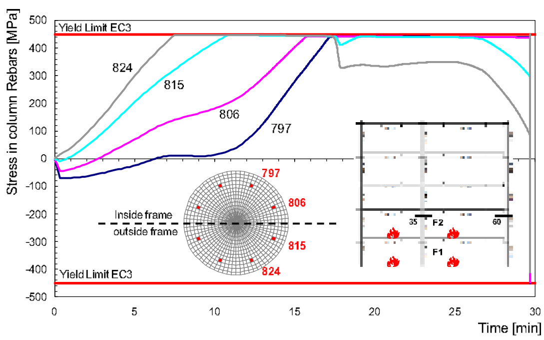

Fig. 11. Top exterior column (60): re-bars stress

The evolution of horizontal displacements at beam ends is shown in Fig. 9; in particular, beams F2 ("damaged") and FB ("undamaged") are compared. The two beams show a quite similar behaviour until the beginning of catenary action; only at this point, the shape of displacements of beam F2 changes completely outlining the tendency of the left side and central columns to deflect inwards since they are pulled by the rapidly bowing down heated beam.
For what concerns the state of stress, several critical cross-sections were investigated [4,9]; in particular, the state of stress in the steel re-bars for the top interior (35) and top exterior (60) columns is shown in Figs. 10 and 11, respectively.
The state of stress in steel re-bars is very high near the connection to the beams probably because the column elements heated on two floors are more flexible and hence subjected to higher displacements. This relieves in some way tensile stresses in the top flanges of heated beams, while the re-bars in the column elements yield quickly in tension.
Further investigation is needed, anyway it seems that for this design scenario, failure was due not only to extensive damage in the heated beams but in the heated columns as well, anyway the frame global behaviour was satisfactory, this achieving a fire resistance rating of nearly 30 minutes and showing a time reduction of 23% with respect to FA and of 20% with respect to FB scenarios.

6 SUMMARY AND ACKNOWLEDGMENT

The presented comprehensive performance-based design methodology had two main goals. The first was integrating seismic and fire design issues since the early stages; the second was providing an assessment method for the evaluation of the post-earthquake fire performance. The application of such a methodology to a suitably defined set of composite frames showed its effectiveness; in fact, the resulting optimized solution showed a satisfactory behaviour with respect to seismic and fire loadings as independent hazards and in the post-earthquake fire situation, as well.
Results presented in this work were obtained in the framework of the following European research project: RFCS Steel RTD Programme, Contract n. RFSR-CR-03034 [3]. Nevertheless the opinions expressed in this paper are those of the writers and do not necessarily reflect those of the sponsors.

REFERENCES

[1] Lee George C., Chen S., Li G., Tong M., On Performance-based Analysis of Buildings for Multi-Hazard Mitigation. *Steel Structures* 4, 231-238, 2004.

[2] Johann A.M., Albano L.D., Fitzgerald R.W., Meacham Brian J., Performance-Based Structural Fire Safety. *Journal of Performance of Constructed Facilities*, Vol. 20, No. 1, pp. 45-53, 2006.

[3] RFCS Steel RTD Programme: PRECIOUS, Prefabricated composite beam-to-column concrete-filled tube or partially reinforced-concrete encased column connections for severe seismic and fire loadings. *Technical Steel Research, Science, Research, Development*. Brussels, 2008.

[4] Alderighi E., Performance of unprotected Composite Frames with Concrete Filled Columns under Seismic and Fire Loadings, *Ph.D. Thesis*, *Dep. of Structural Engineering* Pisa, 2007.

[5] Alderighi E., Braconi A., Salvatore W., Design and performance evaluation of bare steel and composite Moment Resisting Frames subjected to seismic and fire loadings, Proceedings. *XII Italian National Conference on Earthquake Engineering, ANIDIS, Pisa, Italy*. Ed. Plus, 2007.

[6] Alderighi E., Salvatore W., Structural fire performance of earthquake-resistant composite steel–concrete frames. *Engineering Structures* (2009), doi:10.1016/j.engstruct.2008.12.001.

[7] SAFIR. A Thermal/Structural Program Modelling Structures under Fire, Franssen J.-M., *Engineering Journal*, A.I.S.C., Vol 42, No. 3 (2005), 143-158

[8] Alderighi E, Franssen J.M., Salvatore W., Performance of unprotected composite frames with CHS columns submitted to fire loadings. *Eurosteel 2008 - 5th European Conference on Steel and Composite Structures* – Graz (Austria) 3rd-5th September, 2008.

[9] Alderighi E, Franssen J.M., Salvatore W., Post-earthquake structural fire performance of composite steel-concrete frames. *Engineering Structures* (under review),

FIRE ANALYSIS OF STRUCTURES IN SEISMIC AREAS

Raul Zaharia [a], Dan Pintea [a], Dan Dubina [a]

[a] The "Politehnica" University of Timisoara, Romania

INTRODUCTION

Fire following earthquake is the most concerning earthquake-related hazard. In some previous papers [1-4], a state-of-art of the risk management related aspects as well as of the available research concerning the structural aspects of the problem, was presented. On another hand, even in case no fire develops immediately after an earthquake, the possibility of later fires affecting the structure must be adequately taken into account, since the earthquake induced damages make the structure more vulnerable to fire effects than the undamaged one. In the present paper, the authors present a study on the influence of the damage induced by the earthquake and of the collapse mechanism of the damaged or undamaged structures under fire action, on the fire resistance. Both standard and natural fire scenarios are considered. The design fire load density for the natural fire scenarios are determined according to Annex E in EN1991-1-2 [5], considering or not the active fire fighting measures, which could be all available in a normal fire situation, but could be partially available immediately after the occurrence of an earthquake.

1 ANALYSED STRUCTURES

The moment resisting steel plane frames considered for the present study have the dimensions given in *Fig.* 1. The structures are made using European steel profiles of S235 steel grade and all beam-to-column connections are rigid. Both frames were dimensioned for the same fundamental load combinations of actions (4 kN/m^2 for dead load and 2 kN/m^2 for the live load of the current storey, 3.5 kN/m^2 for dead load and 1.5 kN/m^2 for the live load of the top storey, 0.5 kN/m^2 for the wind action). The frames were further verified for two seismic regions in Romania, with different ground motions: a near–field type (Banat region) and a far-field type (Vrancea region). The design was made according to the Romanian seismic code [6], adapted from EN1998. The elastic spectral analysis was applied considering the response spectrum for the Romanian Banat region (moderate seismic area with the design peak ground acceleration a_g=0.16g and control period Tc=0.7 seconds), and for Vrancea region (severe seismic area with the design peak ground acceleration a_g=0.32g and control period Tc=1.6 s). The behaviour factor for the moment resisting frames was considered q=6. The design of the Frame A - Banat structure was governed by the fundamental load combination (no changes in elements dimensions after the seismic design verification). For all other cases (Frame A – Vrancea and Frame B – Banat and Vrancea) the design of the structures was governed by the seismic combination. *Fig.* 1 shows the steel sections of both frames. The values in parathesis represent the profiles used for Vrancea structures, which resulted with stronger beams for some levels and with stronger columns on the height of the building, due to the higher seismic demand.

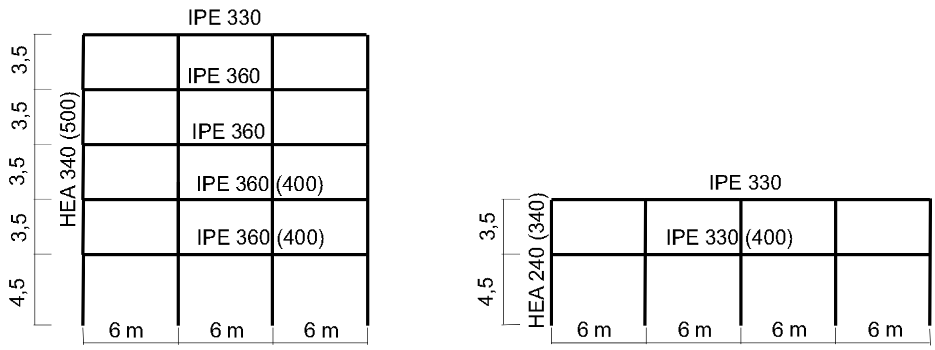

Frame A Frame B

Fig 1. Steel frame dimensions

The seismic response of the structures was evaluated using a pushover analysis, while the displacement demand under the corresponding seismic event was determined using the N2 method [7]. Figures 2-5 show the procedure used to determine the displacement demand (target displacement) of the equivalent SDOF systems for frame B. The entire procedure was presented by the authors in [3].

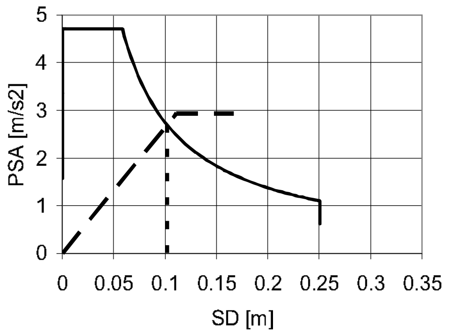

Fig. 2. Seismic demand spectra vs. capacity diagram for Frame A - Banat

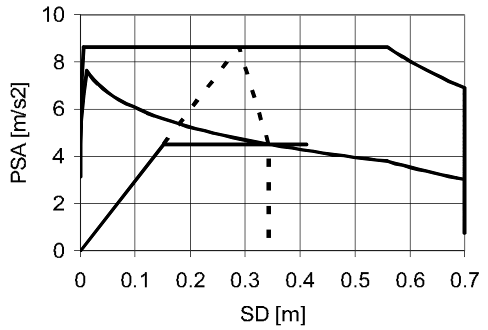

Fig. 3. Seismic demand spectra vs. capacity diagram for Frame A - Vrancea

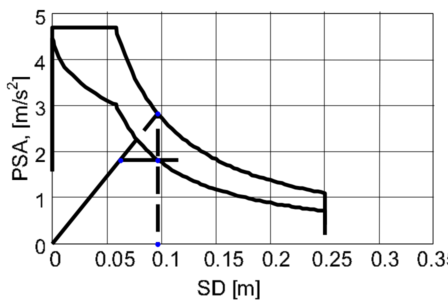

Fig. 3. Seismic demand spectra vs. capacity diagram for Frame B - Banat

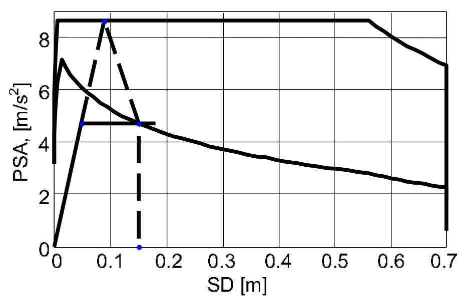

Fig. 4. Seismic demand spectra vs. capacity diagram for Frame B - Vrancea

The Banat Frame A remains elastic after the occurrence of the corresponding earthquake. The Banat frame A was dimensioned from the fundamental load combination, being sensitive to the horizontal wind action, and the steel sections remained the same after the verification for the code seismic action. Frame A - Vrancea responded to the seismic motion in inelastic range, experiencing maximum interstorey drifts of 2.7%, slightly larger than the 2.5% limit corresponding to “Life safety” performance level according to the informative classification given by FEMA 356 [8]. This means that the structure is expected to present important damages of non-structural elements and moderate damages of structural elements, but the safety of the people is guarantied. The same performance level was attained for Frame B (1.8% maximum drifts for Banat frame and 2.2% maximum drifts for Vrancea frame).

Consequently, after the earthquake, the Frame A - Banat structure remains undamaged, while for the other structures in fire analysis, two hypotheses will be considered:

- a lower intensity earthquake occurs and the structure remains undamaged;
- an earthquake with the intensity given by the Romanian code for Banat and Vrancea regions occurs and the structures suffer the damage determined by the above procedure.

2 FIRE ANALYSIS

The standard ISO 834 fire and the natural fires were applied only for the columns and beams of the first storey, in the hypothesis that the ground floor represents a fire compartment. The steel elements have no fire protection. On the beams, the fire was applied on three sides (the top being protected by the concrete slab). In the mechanical analysis, the collaboration between the steel beam and the concrete slab was not considered.

The natural fire curves were obtained using the OZone v2 computer model [9]. Frame A was considered as part of a structure of 18mx18m in plane, while Frame B was considered as part of a structure of 24mx24m. The walls are made out of normal concrete having a thickness of 20 cm, and the following thermal characteristics: conductivity 0.8 W/mK and specific heat of 840 J/kgK. As shown in *Fig. 6* the windows (openings) in three adjacent walls have a sill height of 1 m and a soffit height of 3 m. In the fourth wall the sill height is 2 m and the soffit is 2.5 m. A linear variation of the openings was considered, i.e. the glass panes. At 300°C 30% of the windows were considered broken, while at 500°C all the windows are broken, based on available research presented by the authors in [3, 4].

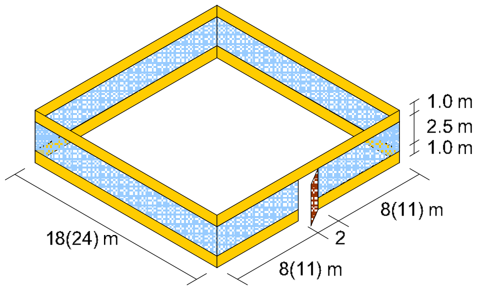

Fig. 6. Fire compartment

The occupancy of the fire compartment is office with a characteristic fire load density $q_{f,k}$ of 511 MJ/m^2. The design fire load density, according to Annex E in EN1991-1-2 [8] is

$$q_{f,d} = q_{f,k} \cdot m \cdot \delta_{q1} \cdot \delta_{q2} \cdot \delta_n \tag{1}$$

in which m is the combustion factor, δ_{q1} is a factor taking into account the fire activation risk due to the size of the compartment (1.51 for frame A and 1.65 for frame B), δ_{q2} is a factor taking into account the fire activation risk due to the type of occupancy (1.00 for both frames - offices) and $\delta_n = \prod_{i=1}^{10} \delta_{ni}$ is a factor taking into account the different active fire fighting measures i (sprinkler, detection, automatic alarm transmission, firemen, etc.).

Table 1 gives the values of the active fire fighting measure factors considered. Before the earthquake, the building being provided with sprinklers, the coefficient which takes into the account the existence of automatic water extinguishing system (δ_1) and the coefficient which takes into account the existence of the independent water supplies (δ_2) are both sub unitary. After the earthquake, considering the possible disruptions, the sprinkler system and the automatic fire detection are no more considered, and the corresponding coefficients are both 1.00. In relation with the prompt intervention of the fire brigades, which is no more possible due to the number of emergencies and traffic congestion, associated to the possible lack of the active fire measures, the coefficients $\delta_{5\text{-}9}$ are considered with the unit value.

Table 1. Fire fighting measures before and after the earthquake

Fire Scenarios	Autom. Water Exting.	Indep Water Supply	Auto Fire Detection	Alarm Fire Brigade	Fire Brigade	Access Routes	Fire Fight Devices	Smoke Exhaust	Total
	δ_1	δ_2	$\delta_{3/4}$	δ_5	$\delta_{6/7}$	δ_8	δ_9	δ_{10}	$\Pi\delta_n$
Before	0.61	0.87	0.73	0.87	0.78	1.0	1.0	1.0	0.26
After	1.0	1.0	1.0	1.0	1.0	1.5	1.5	1.0	2.25

Using these parameters and running the Ozone software [9], two fire curves were produced for each building (*Fig. 7*). For both buildings, the "before earthquake" curves, for which no flashover occurs, are ventilation controlled. The "after earthquake" curves are fuel controlled. The peak temperatures for Frame B are higher than those of the Frame B, due to the higher design fire load density and to the size of the compartment.

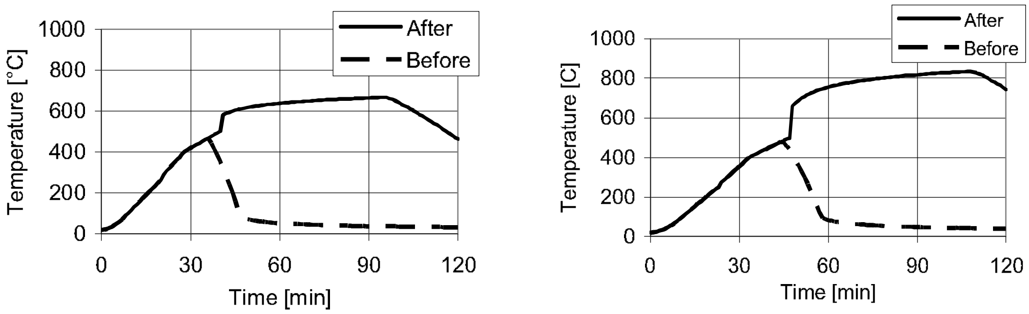

a) Frame A b) Frame B

Fig. 7. Temperature-time evolution

These curves were used in SAFIR programme [10] to find the temperature evolutions on each of the exposed profiles, without fire protection. On the beams the fire was applied on three sides (the top being protected by the concrete slab). In the mechanical analysis, the collaboration between the steel beam and the concrete slab was not considered.
The analysis procedure for damaged structures is shown in figure 8b for the damaged Frame B – Banat under ISO fire. The structure subjected to vertical loads corresponding to the fire load combination is loaded with the lateral forces (push-over by applying an inverted triangular distribution of lateral forces, as described previously) up to the target displacement for the MDOF system, determined using the N2 method. The structure is then discarded of the lateral loads and, because the frame responded in the inelastic range, presents residual displacements. At this stage of structural damage, starts the fire analysis under vertical loads corresponding to the fire load combination. Figure 8 shows the response of both damaged and undamaged Frame-B Banat structure under ISO fire, in terms of displacement – time characteristics.
Two types of collapse modes were observed during the fire analysis using standard or natural fire: a global mode and a mode characterised by the collapse of the beams. For all fire analyses, frame A presented a global collapse mechanism, while frame B presented both modes, as shown in figure 9.

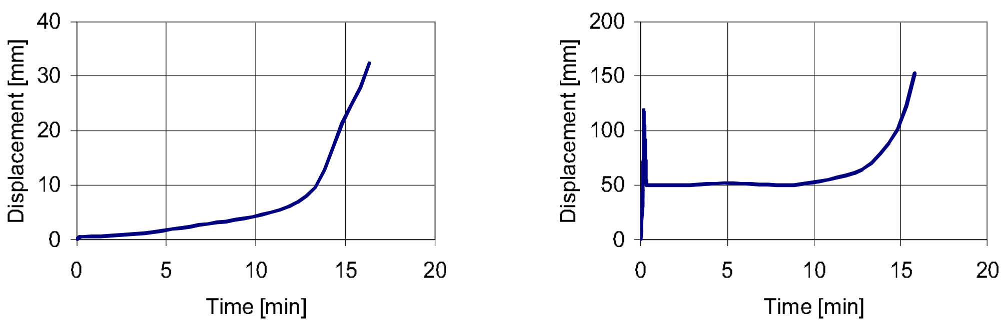

a) Undamaged structure b) Damaged structure

Fig. 8. Displacement-time characteristics for Frame B – Banat under ISO fire

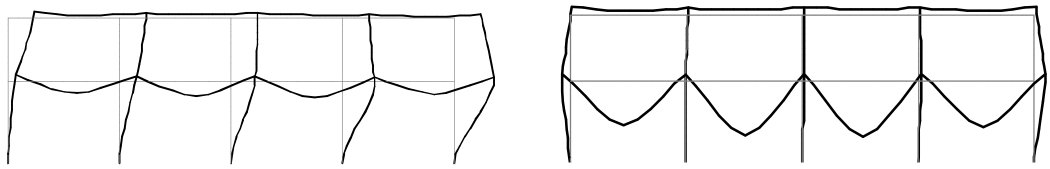

a) Global b) Beam

Fig. 9. Collapse mechanisms for frame B

For all cases, considering all fire fighting measures active (in a situation before an earthquake) both frames, designed for the two seismic regions, resist to the fire action. Therefore, no collapse is produced for "before earthquake" natural fire scenario, for which no flashover occurs. *Table 2* summarizes the fire resistance times and collapse modes for the standard and natural "after earthquake" fire scenarios for each frame.

Table 2. Fire resistance times and collapse modes

ISO fire	Frame A		Frame B	
	Banat	Vrancea	Banat	Vrancea
Undamaged	16' 10" global	26' 10" global	16' 30" global	26' 20" global
Damaged		20' 40" global	15' 40" global	23' 20" global
Natural fire (after earthquake)	Frame A		Frame B	
	Banat	Vrancea	Banat	Vrancea
Undamaged	74' 00" global	no collapse	56' 20" beam	71' 40" beam
Damaged		no collapse	54' 40" global	71' 20" beam

It may be observed that there are important differences of time resistance under standard and natural fire, between the undamaged structures (before earthquake, or for an earthquake of lower intensity than the code seismic action for the corresponding region) and the damaged structures. The differences in fire resistance times between the damaged and undamaged structures are affected by the damage level. Under ISO fire, the differences are ranging from around 5% for the Banat frame B (experiencing maximum inter-storey drifts of 1.8% in the inelastic range), 11% for the Vrancea frame B (experiencing maximum inter-storey drifts of 2.2% in the inelastic range), to around 21% for the Vrancea frame A (experiencing maximum inter-storey drifts of 2.7% in the inelastic range). In case of frame B for Banat region under natural fire, the difference is lower, but it is to be also taken into account that for the damaged and undamaged structures, the collapse mechanism is different. In case of frame B for Vrancea region under natural fire, for both damaged and undamaged structures, the collapse mechanism is local (beam) and the fire resistance time is not influenced in a significant way by the damage of the structure.

For both structures and under both fire scenarios, the Vrancea frame, designed for stronger seismic action, presents higher fire resistance times than the corresponding structures designed for the Banat region. Moreover, in case of frame A, for a natural fire scenario after earthquake, the stronger Vrancea frame resists the fire, even if the structure is damaged after the seismic action, while the Banat frame collapses, even if its structure remains undamaged after the code earthquake.

Therefore, it must be underlined that the structures designed for seismic action (or for stronger seismic action) have an important reserve of resistance into a fire situation.

3 CONCLUSIONS

The study emphasised that there are important differences in time resistance under standard and natural fire between the undamaged structures and the damaged structures, in case of a fire after an earthquake. The fire resistance time of the damaged structures is influenced by the damage level. The highest differences in terms of fire resistance appear between the damaged and undamaged structures experiencing a global type of collapse mechanism. For the fire scenarios with all fire fighting measures available in a regular fire situation, both structures resisted to the fire action (considering all measures available, the fire does not reach flashover). The structures adapted for seismic action, or designed for stronger seismic action, have an important reserve of resistance in case of a fire after an earthquake, but also in case of a regular fire situation.

REFERENCES

[1] Faggiano B., Esposto M., Zaharia R., Pintea D, Risk management in case of fire after earthquake, Urban habitat constructions under catastrophic events, COST Action C26, Malta University Publishing, ISBN 978-99909-44-40-2, 75-80, 2008

[2] Faggiano B., Esposto M., Zaharia R., Pintea D, Structural analysis in case of fire after earthquake, Urban habitat constructions under catastrophic events, COST Action C26, Malta University Publishing, ISBN 978-99909-44-40-2, 75-80, 2008

[3] Zaharia R, Pintea D, Dubina D, Fire after earthquake, Proceedings of the Fifth International Conference Structures in Fire, Singapore, 28-30 May, 2008

[4] Pintea D, Zaharia R, Dubina D, Fire after earthquake- a natural fire approach, Proceedings of the Fifth International Conference EUROSTEEL, 3-5 September, Graz, Austria, 2008

[5] EN1991-1-2: Eurocode 1 - Actions on structures - Part 1-2: General actions - Actions on structures exposed to fire, 2005, European Committee for Standardization, Brussels

[6] P100-1/2004, 2005. Seismic design code – Part 1: Rules for buildings (in Romanian) Indicativ P100-1/2004, Buletinul Constructiilor, Vol. 5, 2005

[7] Fajfar P., A non linear analysis method for performance based seismic design, Earthquake Spectra, vol. 16, no. 3, pp. 573-592, August, 2000

[8] FEMA 356, Guidelines for Seismic Rehabilitation of Buildings, Vol. 1:Guidelines, FEMA 356, Washington DC, 2002 (formerly FEMA 273).

[9] Cadorin, J.F, Pintea, D., Dotreppe, J.C, Franssen, J.M, 2003, A tool to design steel elements submitted to compartment fires- Ozone V2, Fire Safety Journal, Elsevier, 38, 439-451.

[10] J.M. Franssen, VK. R. Kodur, J. Mason, User Manual for SAFIR. A computer program for analysis of structures subbmited to the fire. University of Liege, 2004.

INCOPORATION OF LOAD INDUCED THERMAL STRAIN IN FINITE ELEMENT MODELS

Angus Law[a], Martin Gillie[a], Pankaj Pankaj[a]

[a] The University of Edinburgh, BRE Centre for Fire Safety Engineering, Edinburgh, UK

INTRODUCTION

Load induced thermal strain (LITS) is an integral part of the behaviour of concrete in fire. The existence of LITS has been well documented and modelled by different researchers. It is vital that this strain development is correctly represented in structural models, as the locked in strains due to LITS constituents are significant. Current methods of modelling LITS involve incorporating the strains into constitutive curves. This approach allows the total strains developed due to LITS to be simply included in a finite element analysis. More thorough representation is needed to accurately represent the plastic components in loading directions, and the total strains in non-loading directions. This paper presents a technique to allow the evolution of LITS in accordance with the rules developed in several academic material models [1-3]. The technique is implemented with a simple Drucker-Prager yield surface and the results assessed.

1 CURRENT METHODS

Inclusion of LITS in a concrete constitutive curve is a convenient way of representing LITS in finite element analyses. It allows the modeller to make the LITS constituents temperature dependent and stress dependent – through the use of multiple curves and by giving strains for different stresses respectively. A number of models are available from different sources and for different concretes [1-4]. Failure to represent LITS will result in the modeller not modelling the strains developed in the material accurately, thereby giving an excessively stiff structure. In fact, it could be argued that since LITS is an integral part of concrete behaviour, a modeller failing to include it will not be modelling concrete but some other, non-physical, material.

Once the total strains caused by LITS have been represented, one can then think about the division between elastic and plastic strains. It has been observed that the largest LITS constituents are irrecoverable [5], i.e. they are plastic strains. Therefore, to accurately model these plastic strains it is necessary to determine the elastic modulus of the material as a function of temperature. If the modulus is too stiff, the plastic strains will be overestimated; too soft, and they will be underestimated. The correct modelling of plastic strain constituents becomes increasingly important as a structure cools as the plastic strains will induce greater tension on strain reversal.

Some authors have presented their material models in parts, allowing the user to build the strain constituents into the full curve. The elastic modulus is, therefore, a precisely identifiable constituent of the material model and can be included in a structural model as such; henceforth, this will be termed the “actual” modulus. Other material data such as that presented in the Eurocode do not specify the value of the elastic modulus. In this case, extra care must be taken to represent the strain components accurately. Where the elastic modulus is the initial gradient of the constitutive curve, this will be termed the “apparent” modulus.

2 MULTIPLE DIMENSIONS

The primary focus for research has been on total and plastic strains in the direction of loading. However, attention must also be paid to the non-loading directions. Depending on the model in use, failure to carefully consider the elastic modulus of the material will result in unrepresentative plastic strains, unexpected strains in the non-loading directions, or a mixture of both. The potential for these effects to manifest themselves can be demonstrated by simple example.

2.1 Simple Example

Consider a small cube of concrete, subject to a displacement controlled loading in principle direction 2, but free to move in the transverse directions with a Drucker-Prager yield surface and a perfectly plastic material behaviour, as shown in Figure 1. The associative isotropic flow rule (used here for simplicity) dictates that once the yield surface is reached, plastic strain must occur in a direction orthogonal to the yield surface in stress space. This means that plastic strains are induced in directions other than the one in which the load is applied.

Since the location of trial stress is a function of the elastic modulus, the implications of this for the implementation of LITS via a constitutive curve are significant. The inclusion of LITS whether implicitly (with an “apparent” elastic modulus) or explicitly (with an “actual” elastic modulus) will result in a proportion of that LITS becoming active in the transverse directions. The magnitude of the extra strain would depend on the stress state of the material, and on the degree of plasticity developed in the principle direction. For example: should the element described above be at a stress state at point A, no plastic strains would be induced in the 1-direction.

In the case of the apparent modulus, a large proportion of the extra transverse strain may be elastic; while in the case of the actual modulus, the major constituent of the incremental strain would be plastic.

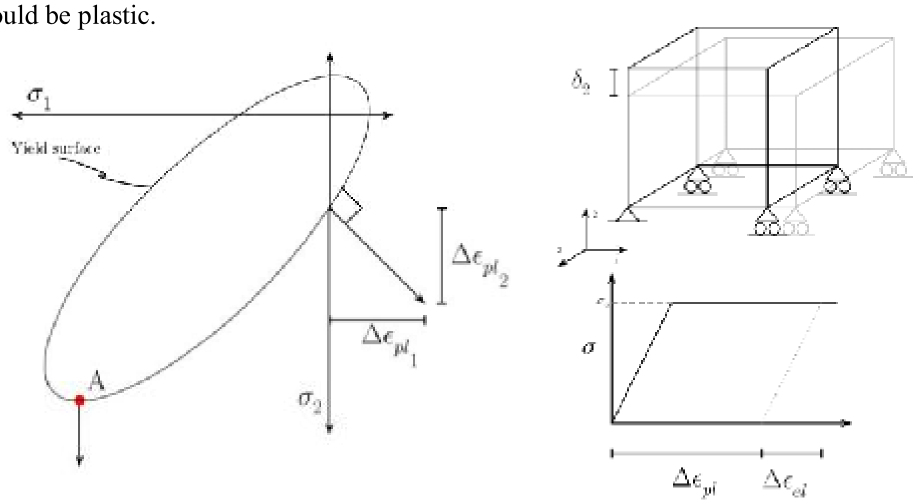

Fig. 1. Plastic flow, and model setup.

The impact of this difference is demonstrated below using the Drucker-Prager yield criterion with a constitutive curve corresponding to that of the 200ºC Terro [2] LITS curve. This temperature was used as there is a significant difference between the actual and apparent moduli, but the temperature is not too extreme. Two different models were created each with a different elastic modulus – apparent or actual – but with the same constitutive curve (Figure 2(a)). The numerical models consisted of a single cubic finite element, restrained at the base in the 2-direction (but free to displace in the 1 and 3-directions) and were strained in the 2-direction. The corresponding deformations and plastic strains were recorded.

Figure 2(b) shows the total strains in the lateral deformation direction. The strains in the 2-direction (i.e. the direction of strain control) are the same for both of the models. In the unrestricted directions, however, there are significant differences in the total strains, particularly in the inelastic phase of the constitutive model. The origin of these differences can be clearly seen from Fig. 2(c). In the "apparent" model the plastic strains do not develop until much later in the deformation process. The "actual" model on the other hand – because of the difference between the elastic modulus and the shape of the constitutive curve – activates the plastic strain constituents immediately. This difference in plastic strain is entirely due to the activation of the flow rule at a much lower stress. Consequently, though the plastic strain in the loading direction is what would be expected from using the "actual" modulus in the constitutive curve, the impact of this approach can be clearly seen in the non-loading directions.

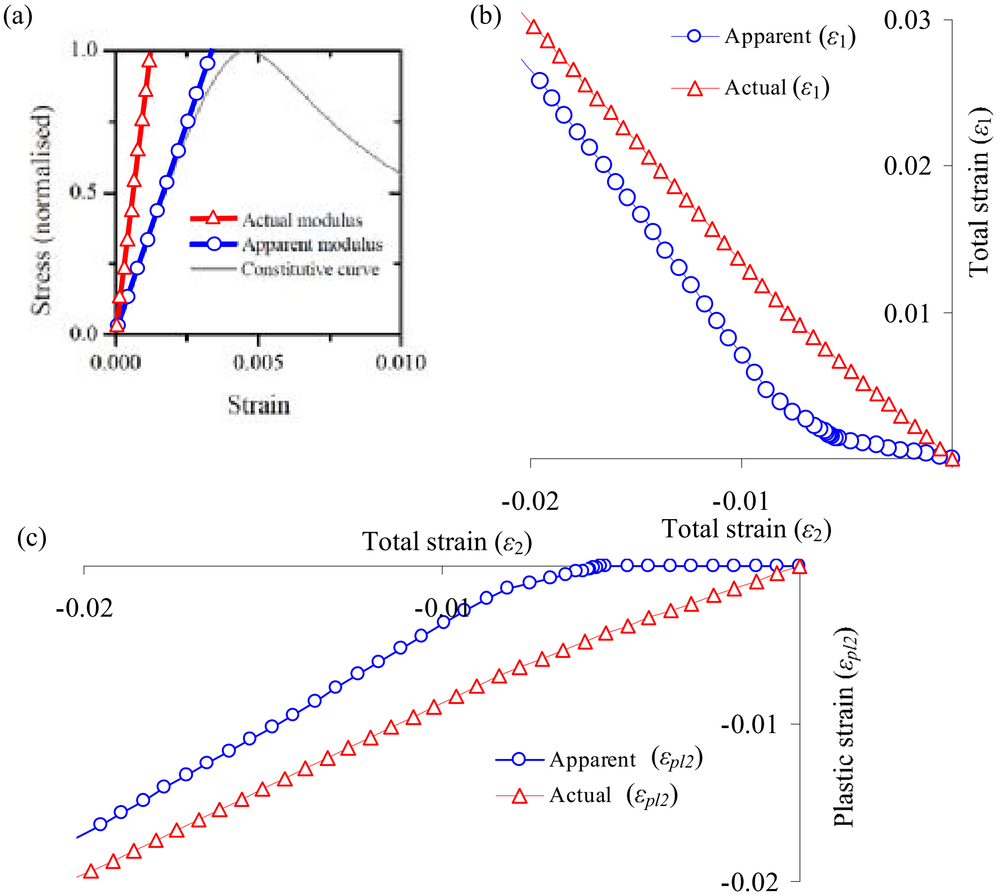

Fig. 2. The same constitutive curve with different elastic moduli gives different lateral deformations and direct plastic strains.

Since equations to represent LITS are all functions of temperature and direct stress, the use of either the apparent or the actual modulus is inadequate if one wants to model the plastic strains accurately, whilst limiting the lateral deformations.

3 THE EMBEDDED MODULUS

To allow the modelling of LITS to be more representative, a new method for the inclusion of LITS in the constitutive model while avoiding the transverse strain issue outlined above is proposed. The Drucker-Prager yield criterion and plasticity equations are solved in a two step method: first, the elastic strains and corresponding plastic strains are calculated using the apparent modulus and the normal solution methods (Figure 3); secondly, the elastic (ε_{el1}) and plastic (ε_{pl1}) strains are recalculated using the actual modulus (Fig. 4). As such, the actual modulus is *embedded* within the solution procedure. This second stage can expressed simply as:

$$\varepsilon_{el1} = \frac{\sigma}{E_{em}} \tag{1}$$

where E_{em} is the embedded actual modulus and σ is the stress calculated from the previous solution. Since:

$$\varepsilon_{el0} + \varepsilon_{pl0} = \varepsilon_{total} \tag{2}$$

where ε_{el0} and ε_{pl0} are the original elastic and plastic strains, and ε_{total} is the total strain. The new plastic strain can be directly calculated from:

$$\varepsilon_{pl1} = \varepsilon_{total} - \varepsilon_{el1} \tag{3}$$

The new plastic and elastic strains are then used in the subsequent analysis. The equivalent plastic strain is not, however, changed. Consequently, the strains developed in the transverse directions are in line with those that would occur when using an apparent modulus, but the plastic strains developed in the principle direction are as would be expected from using the actual modulus. It should also be noted that where plastic strain has occurred, but the yield function is found to be negative (i.e. the total strain is reduced), the corresponding elastic stresses must be recalculated using the embedded modulus. Otherwise, the redistributed strains would be reabsorbed into the elastic region on return to zero stress.

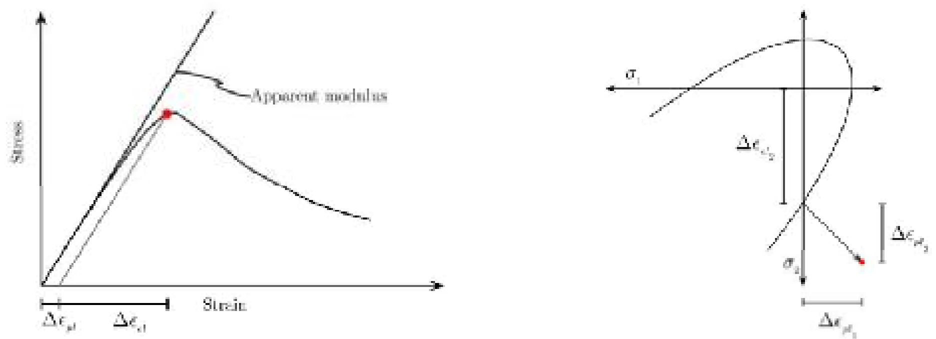

(a) Hardening with apparent modulus

(b) Corresponding strains

Fig. 3. Calculation of plastic and elastic strains.

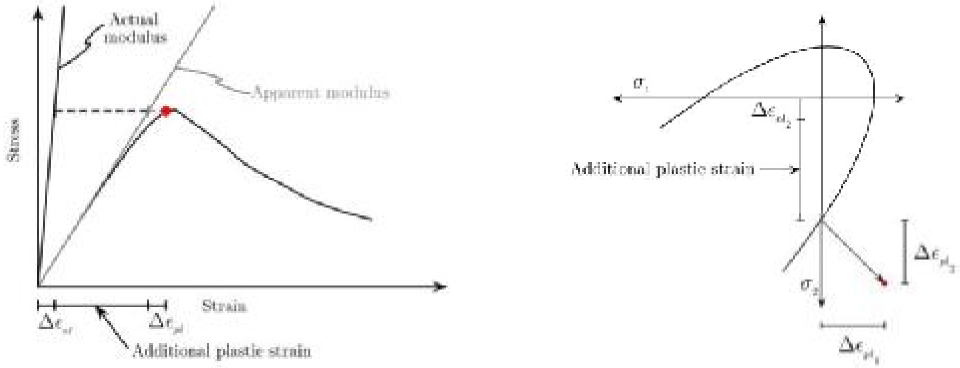

(a) Redistribution found using actual modulus (b) Corresponding strains

Fig. 4. Redistribution of strains due to the difference between actual modulus and apparent modulus.

A Drucker-Prager model was created [6-12] which incorporated this method of modification by the embedded modulus. A model with an apparent elastic modulus and an embedded actual modulus was subjected to the previously described test. The results were compared with the previous models (Figure 5).

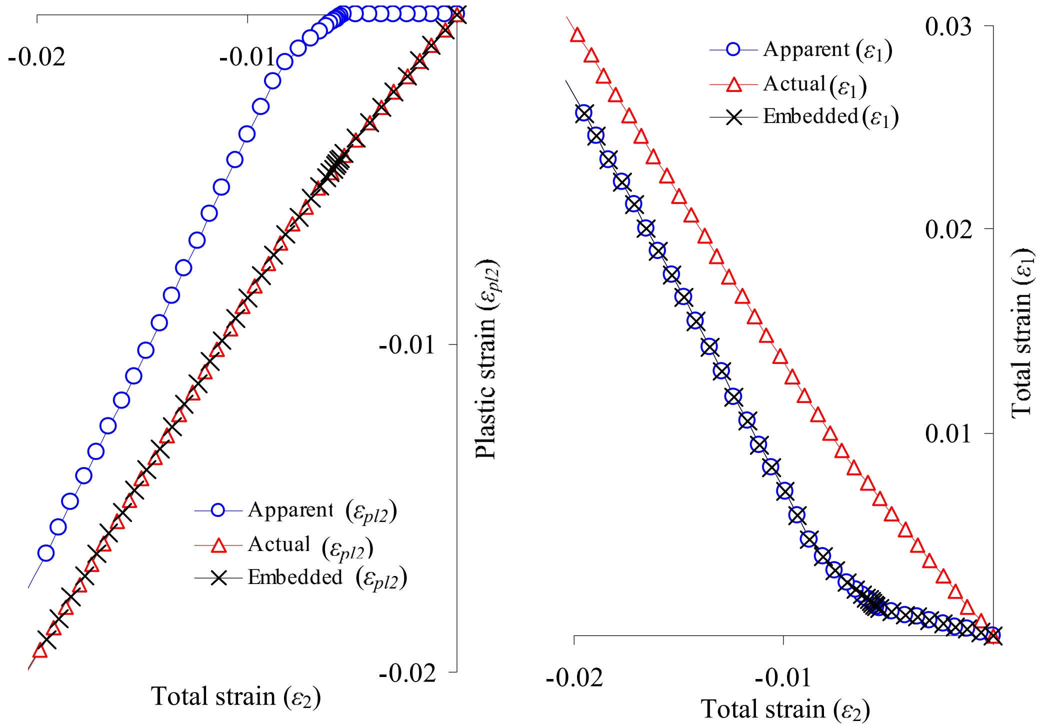

Fig.5. Comparison of two stage approach with results from original models.

The total lateral strains experienced by the "embedded" material are the same as those experienced by the "apparent" material. Equally, the total plastic strain experienced in the loading direction is the same as those experienced by the "actual" material. Thus, a fully plastic, transient strain constituent has been included in the model without affecting the deformations in the non-loading directions. This allows the plastic LITS effect to be successfully modelled uni-axially and in proportion to the applied stress in the way stated in the governing LITS equations.

4 CONCLUSION

There are several conclusions to be drawn from this study:

- There are significant differences between a constitutive curve which includes LITS, and a full constitutive model which accurately represents LITS components.
- Inclusion of the plastic strains by means of an "apparent" modulus is useful in one dimension; however, plastic flow rules cause unwanted strains to develop laterally when more than one dimension is considered
- Use of a two step model with an "apparent" modulus, and an embedded "actual" modulus within the material model is one approach which can be used to correctly model the plastic strain due to the LITS equations, while allowing the strain in the lateral directions to be modelled correctly. This model has been demonstrated in the case of an element deformed uniaxially.

The authors of this work would like to gratefully thank the project sponsors; BRE Trust, and the EPSRC.

5 REFERENCES

[1] Anderberg Y, Thelandersson S: Stress and Deformation Characteristics of Concrete, 2 - Experimental Investigation and Material Behaviour Model. Sweden, University of Lund, 1976

[2] Terro MJ: Numerical Modeling of the Behaviour of Concrete Structures in Fire. *ACI Structural Journal 95:183-193*, 1998

[3] Nielsen CV, Pearce CJ, Bicanic N: Theoretical Model of High Temperature Effects on Uniaxial Concrete Member under Elastic Restraint. *Magazine of Concrete Research 54:239-249*, 2002

[4] EN1992-1-2: Design of Concrete Structures - Part1-2: General Rules- Structural Fire Design, 1992

[5] Khoury GA, Grainger BN, Sullivan PJE: Transient Thermal Strain of Concrete: Literature Review, Conditions within Specimen and Behaviour of Individual Constituents. *Magazine of Concrete Research 37:131-144*, 1985

[6] Calladine CR: Plasticity for Engineers: Theory and Applications. Chichester, Horwood Publishing, 2000

[7] Crisfield MA: Non-Linear Finite Element Analysis of Solids and Structures. Chichester, Wiley, 1991

[8] Crisfield MA: Non-Linear Finite Element Analysis of Solids and Structures: Advanced Topics. Chichester, Wiley, 1997

[9] Cook RD, Malkus DS, Plesha ME, *et al.*: Concepts and Applications of Finite Element Analysis. Chichester, Wiley, 2002

[10] Hill R: The Mathematical Theory of Plasticity. Oxford, Oxford University Press, 1950

[11] Pankaj: Finite Element Analysis in Strain Softening and Localisation Problems, in Department of Civil Engineering. Swansea, University College of Swansea, 1990

[12] Zienkiewicz OC: The Finite Element Method (ed 3). London, McGraw-Hill, 1977

FIRE RESISTANCE ASSESSMENT FOR DIFFERENTIATED SAFETY REQUIREMENTS

Mariusz Maślak [a]

[a] Cracow University of Technology, Faculty of Civil Engineering, Cracow, Poland

INTRODUCTION

Classical methodology of structural member fire resistance evaluation, proposed by the standard EN 1991-1-2 [1], is connected with a comparison between the design value of unfavourable action effect $E_{fi,d,t}$ of a combination of external loads applied to the structure together with internal forces and moments induced as a result of thermal strains constrainment, and the design value of resistance $R_{fi,d,t}$, reduced in high temperature. In such an approach the fire resistance limit state is reached if $E_{fi,d,t} = R_{fi,d,t}$. In the present paper the safety level of simply supported steel floor beam is studied for fire situation. Such elementary example is selected specially for simplicity and clarity of the interpretations. The permanent load $g[kN/m]$ as well as the only one variable load $q[kN/m]$, both uniformly distributed, are applied to the member. The bending moment, calculated according to the rules of accidental design situation, can be considered as a conclusive action effect:

$$E_{fi,d,t} = M_{fi,d,t} = \left(g_k + \gamma_Q \psi_2 q_k\right) L^2 / 8 \tag{1}$$

where $L[m]$ is the span length, γ_Q is the partial safety factor defined for variable loads, and $\psi_2 q_k$ is a quasi-permanent value of variable action (in some countries a frequent value of this action $\psi_1 q_k > \psi_2 q_k$ is suggested to be used). Let us notice that the value of $E_{fi,d,t}$ remains constant during the whole fire time provided that the beam has the possibility of unlimited thermal deformation. In reality this is only the approximation because load changes generated by evacuation of building occupants or furnishings combustion are not taken into consideration in the analysis. Design value of member resistance $R_{fi,d,t}$ is obtained based on its characteristic value $R_{fi,k,t}$. In fact $R_{fi,d,t} = R_{fi,k,t} / \gamma_{M,fi}$; however, a suggestion to accept $\gamma_{M,fi} = 1{,}0$ is given in the standard [1]. In simple load cases $R_{fi,k,t}$ is proportional to steel yield point $f_y = f_{y,k} [MPa]$. The bending modulus W is adopted as a proportionality factor in the considered example. When steel temperature $\Theta_a [^oC]$ grows, f_y decreases as follows:

$$f_{y,\Theta} = k_{y,\Theta} f_{y,20} \tag{2}$$

The quantity $f_{y,20}$, defined for the room temperature $\Theta_a = 20^o C$, is then understood as a reference value. Parameter $k_{y,\Theta}$ is a suitable reduction coefficient. Its values, determined for particular steel temperatures, are given in EN 1993-1-2 [2]. Finally, the beam resistance can be calculated by means of the following formula:

$$R_{fi,d,t} = R_{fi,k,t} / \gamma_{M,fi} = W k_{y,\Theta} f_{y,20} \tag{3}$$

1 REQUIRED SAFETY LEVEL

Failure probability p_f is usually adopted as the reliable safety measure in design of steel members for fire situation. If maximum value of such probability, acceptable by the user of the structure, is described as $p_{f,ult}$, then the global safety condition has the following form:

$$p_f < p_{f,ult} \tag{4}$$

This formula is frequently rearranged to the equivalent inequality:

$$\beta > \beta_{req} \tag{5}$$

in which β is the global reliability index. Its required (target) value β_{req} is explicitly connected with ultimate failure probability. If random variables E and R are described by means of normal or log-normal probability distribution, then:

$$p_{f,ult} = \Phi(-\beta_{req}) \rightarrow \beta_{req} = -inv\Phi(p_{f,ult}) \tag{6}$$

Symbol $\Phi(\,)$ means the cumulative distribution function of standardized normal probability distribution. The notation $inv\Phi$ is understood as an inverse function of Φ. Probability $p_{f,ult}$ is unequivocally determined only if corresponded reference period $n[years]$ is given. Usually it is assumed that $n = 50\,years$; however, period $n = 1\,year$ is also considered in many cases. In general, if the probability $p_{f,ult}$ identified within 50 years period is known, then its respective value, adequate for $n \neq 50\,years$, may be calculated from the equation:

$$\Phi(\beta_{50}) = 1 - \Phi(-\beta_{50}) = \Phi(\beta_n)^{50/n}\text{, hence if } n = 1\,year \text{ we have: } \Phi(\beta_1)^{50} = \Phi(\beta_{50}) \tag{7}$$

Values of β_{req} are differentiated depending on real safety requirements. Such a methodology leads to the specification of various kinds of reliability classes RC. They are the most frequently related to the consequences of failure or to the relative cost of safety measure [3]. In the standard EN 1990 [4] only three reliability classes are defined (Table 1).

Table 1. Reliability classes according to EN 1990 [4]

Reliability class	Safety requirements	β_{req} for reference period equal:	
		one year	50 years
RC3	range	$\beta_{1,req} = 5{,}2\ (p_{1,f,ult} \approx 9{,}9 \cdot 10^{-8})$	$\beta_{50,req} = 4{,}3\ (p_{50,f,ult} \approx 8{,}5 \cdot 10^{-6})$
RC2	moderate	$\beta_{1,req} = 4{,}7\ (p_{1,f,ult} \approx 1{,}3 \cdot 10^{-6})$	$\beta_{50,req} = 3{,}8\ (p_{50,f,ult} \approx 7{,}2 \cdot 10^{-5})$
RC1	minor	$\beta_{1,req} = 4{,}2\ (p_{1,f,ult} \approx 1.3 \cdot 10^{-5})$	$\beta_{50,req} = 3{,}3\ (p_{50,f,ult} \approx 4{,}8 \cdot 10^{-4})$

2 PARTIAL SAFETY FACTOR FOR VARIABLE LOADS

The component safety factor γ_Q specified for variable load is the basic safety measure necessary to obtain design value of the action effect $E_{fi,d,t}$ (see Eq. 1). Its constant value $\gamma_Q = 1{,}5$ is accepted in design methodology based on the standard recommendations. However, such statement is not precise enough. In reality, its minimum value $\gamma_{Q,\min}$ is greater for greater coefficient v_Q. Action q applied to the beam is a random variable described by means of *Gumbel* probability distribution $G(\tilde{q}, u_Q)$ - $\tilde{q}$ is the modal value of load intensity whereas u_Q is *Gumbel* standard deviation. It is well known that:

$$u_Q = \sigma_Q \sqrt{6} / \pi = 0{,}78\sigma_Q \quad \text{and} \quad \tilde{q} = \bar{q} - 0{,}577 u_Q = \bar{q} - 0{,}45\sigma_Q \tag{8}$$

where $\bar{q}$ and σ_Q are the parameters of normal probability distribution - the mean value and the standard deviation, respectively. Design load intensity q_d depends on the component value of global safety index $\beta_E = \alpha_E \beta$ (it is a partial safety index determined for the action effect). Ultimate limit state is reached if $\beta = \beta_{req}$. Furthermore, according to design format proposed by [4] constant value $\alpha_E = 0{,}7$ is fixed as a result of calibration process presented in many papers. Finally, for *Gumbel* probability distribution, we have:

$$q_d = \tilde{q} - u_Q \ln[-\ln \Phi(\alpha_E \beta)] = \bar{q}\{1 - 0{,}78 v_Q [0{,}577 + \ln(-\ln \Phi(0{,}7\beta))]\} \tag{9}$$

where $v_Q = \sigma_Q / \bar{q}$. Characteristic value q_k is defined as a 95% fractile, therefore:

$$q_k = \tilde{q} - u_Q \ln[-\ln(0{,}95)] = \bar{q}\{1 - 0{,}78 v_Q [0{,}577 + \ln(-\ln(0{,}95))]\} = \bar{q}(1 + 1{,}867 v_Q) \tag{10}$$

Consequently:

$$\gamma_Q = \frac{q_d}{q_k} = \frac{1 - 0{,}78 v_Q \{0{,}577 + \ln[-\ln \Phi(0{,}7\beta)]\}}{1 + 1{,}867 v_q} \tag{11}$$

Substituting particular values of $\beta_{50,req}$ and $\beta_{1,req}$ from Table 1 into the place of β in Eq. 11 gives the set of functions $\gamma_{Q,\min} = \gamma_{Q,\min}(v_Q)$ presented in Fig. 1a for 50 year and in Fig 1b for one year reference periods. They are the minimum values of γ_Q for which the component safety condition $E_{fi} < E_{fi,d,t}$ (its equivalent is the inequality $\beta_E \geq \beta_{E,req} = 0{,}7\beta_{req}$) is satisfied. Let us notice that the standard value $\gamma_Q = 1{,}5$ is in general much greater than $\gamma_{Q,\min}$, even if the range safety requirements are assumed and load variability is considerable ($v_Q \geq 0{,}2$).

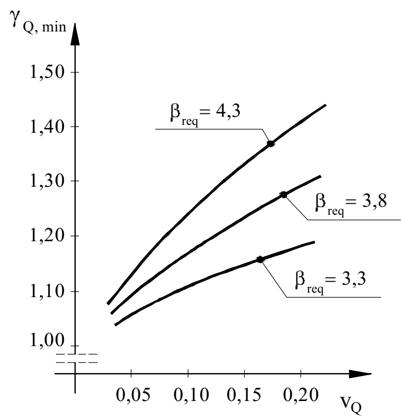

Fig.1a. Minimum values of γ_Q for 50 year reference period

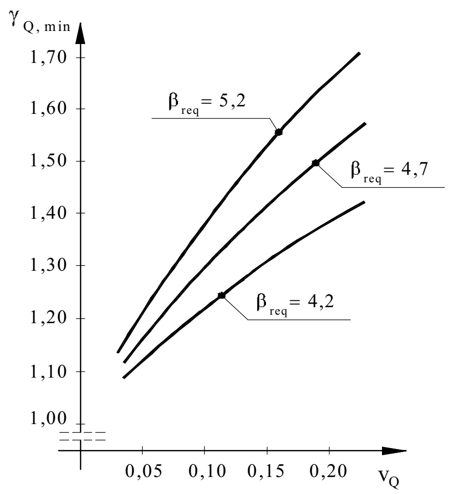

Fig.1b. Minimum values of γ_Q for one year reference period

3 LIMITATIONS RELATED TO MEMBER RESISTANCE

Analogous condition $R_{fi} > R_{fi,d,t}$, in other words $\beta_R > \beta_{R,req} = \alpha_R \beta$, leads to the specification of minimum values of partial safety factor $\gamma_{M,fi}$. In the standard [4] a constatnt value $\alpha_R = 0{,}8$ is suggested. Random variable R is characterized by log-normal probability distribution $LN(\breve{R}, \upsilon_R)$ - $\breve{R}$ is the median value, whereas υ_R - the log-normal coefficient of variation. Characteristic value $R_{fi,k,t}$ is assumed as a 95% fractile. Consequently:

$$\gamma_{M,fi} = \frac{R_{fi,k,t}}{R_{fi,d,t}} = \frac{\breve{R}\exp(-1{,}645\upsilon_R)}{\breve{R}\exp(-0{,}8\beta\upsilon_R)} = \exp[(0{,}8\beta - 1{,}645)\upsilon_R] \tag{12}$$

Taking particular $\beta_{50,req}$ from Table 1 as a β value in Eq. 12 gives curves $\gamma_{M,fi,\min} = \gamma_{M,fi,\min}(\upsilon_R)$ presented in Fig. 2. Let us underline that those values are always greater than constant value $\gamma_{M,fi} = 1{,}0$ proposed in [1] and [2].

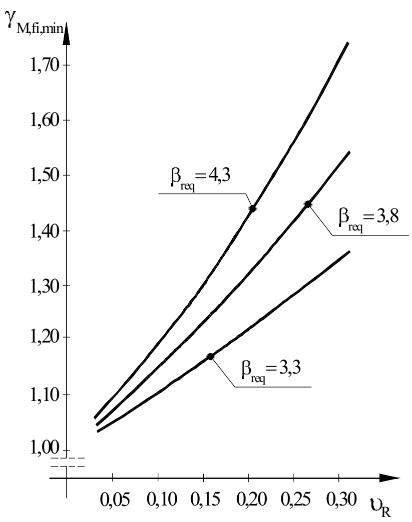

Fig. 2. Minimum values of $\gamma_{M,fi}$

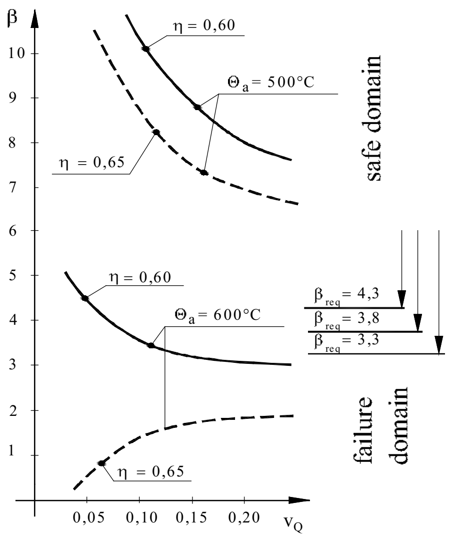

Fig. 3. Global reliability index $\beta = \beta(v_Q)$ for selected temperatures of steel

4 GLOBAL SAFETY CONDITION

Basic safety condition has the form $E_{fi,d,t} < R_{fi,d,t}$. It means that the safety margin can be calculated as $g = R_{fi} - E_{fi} > 0$, hence in ultimate limit state we have:

$$g = R_{fi,d,t} - E_{fi,d,t} = 0 \tag{13}$$

Let $\eta = q_k/(g_k + q_k)$ be the parameter which reflects the importance of variable action in relation to the total load. Value $\eta = 0$ means that $q_k = 0$, on the other hand if $\eta = 1$ then $g_k = 0$. Furthermore $\breve{R} = \breve{W}\breve{k}_y\breve{f}_y$, where $\breve{f}_y = f_{y,k}\exp(2\upsilon_f)$ - as a 98% fractile, $\upsilon_f = 0{,}08$ (it is a measure of variability of f_y), $\breve{k}_y$ is adopted as a nominal value k_y from [2], $\breve{W}$ is also equal to the nominal value taken from tables. Random variability of k_y and *W*, described by means of the coefficients υ_k and υ_A respectively, is summed with υ_f giving $\upsilon_R = \sqrt{\upsilon_f^2 + \upsilon_A^2 + \upsilon_k^2}$. It is accepted that $\upsilon_A = 0{,}06$ and $\upsilon_k = 0{,}20$, then $\upsilon_R = 0{,}22$. Such a great value of variability of k_y is the reflection of considerable uncertainty of a model describing mechanical properties of steel under fire conditions. For example *M. Holicky* [5] suggests to use in this field $\upsilon_k = 0{,}10 \div 0{,}30$. Finally, Eq. 13 can be rearranged to the form:

$$g(\eta, \Theta_a, \beta, \upsilon_R, v_g, v_Q) = R_{fi,k,t} - \left(\frac{g_k \cdot L^2}{8}\right)\left(1 + \gamma_Q \psi_2 \frac{\eta}{1-\eta}\right) = 0 \qquad (14)$$

This condition has been solved for the beam made of IPE300 and the span length equal $L = 6m$. Many diagrams can be presented as a result of such calculation. Dependence between the index β and coefficient v_Q, determined for selected temperatures Θ_a, is given in Fig. 3. Functions $\beta = \beta(v_Q)$ specified for particular values of η parameter are shown in Fig. 4 (for $\Theta_a = 400^o C$ in Fig. 4a, and for $\Theta_a = 600^o C$ in Fig. 4b). Last of all, curves $\beta = \beta(\eta)$ are demonstrated in Fig. 5 for various temperatures Θ_a (let us notice that variability $v_Q = 0{,}1$ is adopted in Fig. 5a, whereas $v_Q = 0{,}2$ in Fig. 5b). It is extremely important that all values of β index, obtained from Eq. 14 and presented in Figures 3, 4 and 5, have to be compared with suitable levels of safety margin, which are defined by the ultimate values of β_{req} (those levels are marked separately in analysed diagrams).

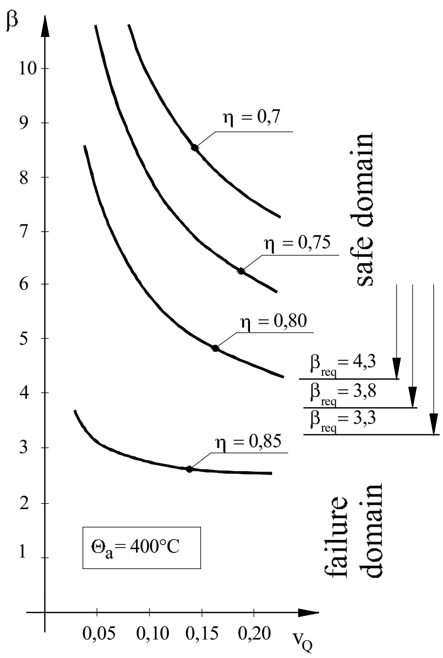

Fig. 4a. Reliability index $\beta = \beta(v_Q)$ for particular values of η parameter ($\Theta_a = 400^o C$)

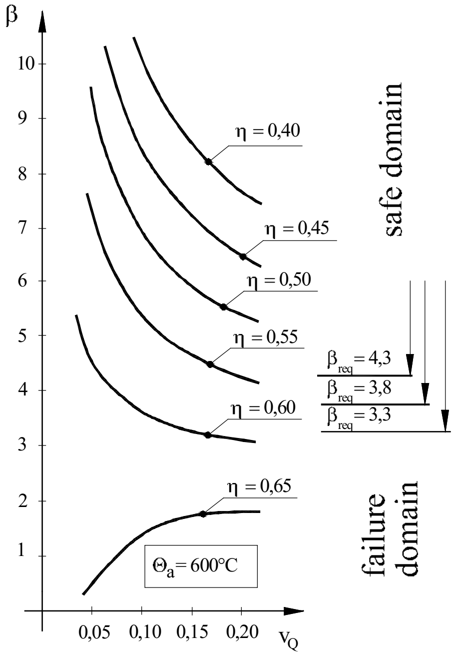

Fig. 4b. Reliability index $\beta = \beta(v_Q)$ for particular values of η parameter ($\Theta_a = 600^o C$)

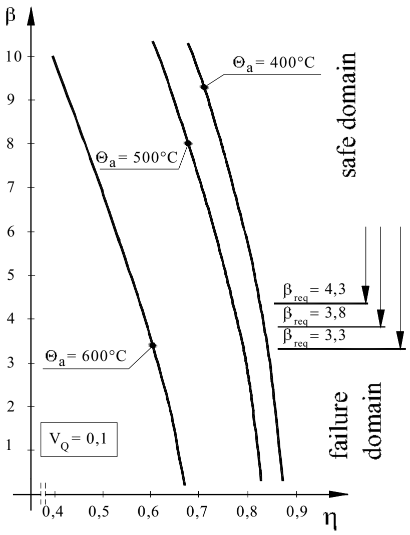

Fig. 5a. Reliability index $\beta = \beta(\eta)$ for selected temperatures of steel ($v_Q = 0{,}1$)

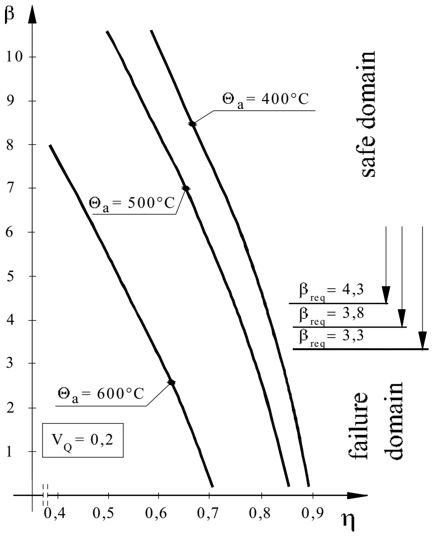

Fig. 5b. Reliability index $\beta = \beta(\eta)$ for selected temperatures of steel ($v_Q = 0{,}2$)

5 SUMMARY AND CONCLUSIONS

The aim of this paper is to show the ratio of the transformation of real safety level during fire. The global reliability index β is adopted as a reliable measure which allows to determine the member failure probabilty p_f in particular fire moments described by means of different steel temperatures Θ_a. Not only the global safety condition $E_{d,fi,t} < R_{d,fi,t}$ but also two component limitations: $E_{fi} < E_{fi,d,t}$ and $R_{fi} > R_{fi,d,t}$, have to be taken into account in such semi-probabilistic design approach. Inserted figures show the functions $\beta = \beta(v_Q)$ and $\beta = \beta(\eta)$ and their dependence on steel temperature growth. Differentiated safety requirements are considered due to the specification of various reliability classes which is an equivalent of the acceptance of different values of required index β_{req}. The simplified design aproach proposed by standards [1] and [2] is not fully compatible with classical methodology of member safety evaluation. In the present paper it is shown that the suggested value $\gamma_{M,fi} = 1{,}0$ is too small to secure required safety level of the resistance. On the other hand, this lack is partly compensated by the acceptance of constant value $\gamma_Q = 1{,}5$, greater then necessary.

REFERENCES

[1] EN 1991-1-2, Eurocode 1: Action on structures – Part 1-2: General actions – Actions on structures exposed to fire,

[2] EN 1993-1-2, Eurocode 3: Design of steel structures – Part 1-2: General rules – Structural fire design,

[3] JCSS Probabilistic Model Code, Joint Committee on Structural Safety, 2001,

[4] EN 1990, Eurocode – Basis of structural design,

[5] Holicky M., Decision on fire safety measures based on risk assessment, Proceedings of 9th International Conference on Structural Safety and Reliability *ICOSSAR*, Rome, Italy, June 19-23, 2005.

PERFORMANCE OF STRUCTURAL SYSTEMS IN FIRE

H. Mostafaei , M. A. Sultan, N. Bénichou
National Research Council Canada, Institute for Research in Construction, Ottawa, Canada

INTRODUCTION

Traditionally, fire-resistance tests of structures have been employed based on individual element tests and without consideration of interactions among structural elements and systemic structural response. Recent studies indicate that systemic interactions and boundary conditions of a structure can have significant effects both on the performance of the entire structural system and on the response of the individual structural elements. Therefore, to achieve a comprehensive understanding of the structural response, application of a proper performance-based evaluation and design methodology is inevitable.

One of the most important systemic phenomena, barely considered previously in the design of building structures exposed to fire, is the effect of thermal expansion on the behaviour of structures in fire [1]. Effects of thermal expansion on structural performance could not be evaluated based on the traditional fire-resistance tests, in which structural elements such as beams, floors, or columns, are exposed to the standard fire, individually, disregarding the boundary conditions. Therefore, to investigate the behaviour of structures subjected to thermal expansion, a performance-based evaluation approach would be perhaps the best methodology to apply.

Thermal expansion is not a new term in structural engineering, as it has been considered in the design of bridge structures for many years at ambient temperature. However, such consideration has not been extended to the design of building structures exposed to fire. A recent study on the collapse of World Trade Centre Building 7 revealed that thermal expansion has a major effect on the structural response and can induce even progressive collapse of a structure [1]. A study on the results of survey on several past collapses of moderate-high building structures [2] revealed the fact that most of these structural failures seem to share a similar pattern of collapse with significant thermal expansion effects on the structural performance. Results of the studies on the collapse of structures in fire, such as the World Trade Center Towers, illustrate a collapse sequence in which the elevated temperature due to fire causes initial thermal expansion of the building floors following by the floors sagging and pulling inward on the exterior columns, resulting in a progressive collapse of the buildings [3,4].

These recent research findings indicate two important issues; 1) thermal expansion plays a very important role in the performance of structures in fire, and 2) to simulate and assess realistic 3D structural response of structures in fire, performance of the entire structural system should be investigated using a proper performance-based evaluation methodology and technique.

The objective of this article is to provide results of a literature review on the performance evaluation of buildings in fire considering the effects of thermal expansion, structural systems and material properties. As a result of this study, new avenues for future research on collapse mitigation of structures in fire are identified and suggested.

1 THERMAL EXPANSION

One of the major terms that should be considered in the design of large-scale structures, such as bridges, is the thermal expansion of the structures. For bridges, for instance, this will result in the design of thermal expansion joints located along the bridge deck, which seems to be one of the most effective solutions to mitigate effects of thermal expansion on the deck due to variation of ambient temperature through the year. As for building structures, thermal expansion due to ambient temperature has not been a major design concern. However, when it comes to structural performance exposed to fire, thermal expansion would play a major role in the response and behaviour of structures. Recently, the National Institute of Standards and Technology of the United States has revealed results of a study on the collapse assessment and simulation of World Trade Centre Building 7 [5], concluding:

"Thermal expansion is a new phenomenon that can cause structural collapse. For the first time we have shown that fire can induce a progressive collapse. Currently thermal expansion effects are not explicitly considered in design practice for fire resistance ratings."

This result reveals the fact that currently, there is a clear lack of knowledge and design methodology relating to the effects of thermal expansion on performance of structures in fire. Furthermore, results from previous experimental studies [6], and from observed collapses of structures in fire [2], also indicate that such structures can experience significant floor expansion at high temperatures inducing large lateral deformation or drift to columns or resulting in floor sagging in compression. These, in turn, can result in the collapse of partial or entire structures.

Fig. 1 illustrates a photo taken after a major fire at the US Military Personnel Records Centre building [2]. This photo shows a lateral deformation of about 60 cm for a column on the sixth floor of the building induced by the floor expansion due to the fire. In fact, this is very similar to a reinforced concrete column failure under extreme lateral loads such as earthquakes. This deformation is the result of floor thermal expansion during the fire. Usually temperatures at the ceiling level of the fire compartment are much higher than that at the floor level of the compartment. This temperature difference induced different thermal expansions for the floors at the upper and lower levels, which resulted in a significantly larger deformation at the top of the columns compared to the base causing significant shear forces and end moments on the elements. If the induced drift to the element exceeds the upper bond of the column deformation capacity, it will fail either in shear or buckling.

Fig. 1. Large drift and shear failure of a column due to thermal expansion of floor [2]

In the case of the US Military Personnel Records Centre building, shown in Fig. 1, the column drift is significantly larger than the shear deformation capacity of the element and a clear shear failure occurred at the top of the column. Such column response and failure mode could not be predicted using the traditional column furnace test method, in which a single column is exposed to a standard fire and subjected to only constant axial load.

Lateral deformations of columns due to floor thermal expansion have also been observed in a full-scale fire test [6]. Previously, a full-scale reinforced concrete building in fire was tested at the Cardington test facility of BRE, UK. Fig. 2 shows a plan of first floor of the building, fire compartment location, and burning of the fire compartment. During the test, lateral deformations of the floor at the top of the first floor columns have been measured, shown also on the floor plan in Fig. 2. The maximum lateral deformation at the first floor measured during the fire was about 67 mm. This is still a relatively large lateral deformation and drift induced on the columns. This deformation compared to that of the column at the US Military Personnel Records Centre is relatively small. This is mainly because of the small size of the fire compartment and the floor dimensions. Typically the larger the floor size is the larger thermal expansion and lateral deformation can occur. Practically, floor size of conventional moderate-rise buildings is relatively larger than that of the building specimen in Fig. 2. This in fact could be one of the reasons that thermal expansion effect has been hardly observed in previous moderate or small size tests.

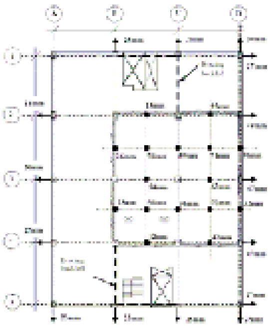

Fig. 2. Fire test of a full-scale reinforced concrete building, 2001 (BRE) Cardington [6]

The National Institute of Standards and Technology of the United States reported 22 fire-induced multi-story building collapses since 1970; fifteen cases were from the USA, two from Canada, and 5 from Europe, Russia and South America [2]. Out of the 22 building collapses, 7 buildings had reinforced concrete structures, 6 steel frames, 5 masonry systems, 2 wood structures and 2 unknown materials. A study on these building collapses could reveal that the main reason for most of these building collapses could be not only due to strength degradation of the materials exposed to elevated temperature but also to the significant effects of thermal expansion on the entire structural performance and thermal stresses and strains on the individual elements. Therefore, further studies are recommended to investigate the behaviour of structures in fire considering the effects of thermal expansion.

2 REINFORCED CONCRETE STRUCTURES IN FIRE

Reinforced concrete structures have been categorized as structures with very good reliability and fire resistance properties. As mentioned in the previous section, surprisingly, the National Institute of Standards and Technology of the United States reported the largest number of collapses of structures among conventional structures, since 1970, belonged to reinforced concrete buildings [2]. This would be mostly due to the brittle nature of concrete materials. However, there is currently a significant lack of information and analytical tools for performance evaluation ad design of reinforced concrete structures especially under design fire, realistic loading and failure scenarios [7].

A failure mechanism of reinforced concrete structures in fire is the loss of capacity due to spalling of cover concrete resulting in failure of the element or sometimes even partial or the entire structure. The phenomenon of spalling is very complex and not well understood. Experiments have shown that spalling of cover concrete exposed to fire is essentially due to high moisture content, high rates of heating, and high concrete stresses [8,9]. There are studies showing that spalling rate is dependant on the size of the elements and specimen

scales [10]. The type of aggregate also has some effects on the mechanical properties and spalling of concrete. Spalling is generally much less for carbonate aggregate concrete compared to that of siliceous aggregate concrete [11]. Studies show, spalling of high strength concrete is considerably higher than that for normal strength concrete exposed to fire, as shown in Fig. 3. This is in fact referred to as one of the major concerns with high strength concrete, which could be due to its low water/cement ratio [12]. Recent studies on post-tensioned structures such as post-tensioned beams and slabs have revealed that the effect of spalling on these structural elements can be very significant and could result in the collapse of the structure. Further studies in this area are urgently suggested [13].
The issue of thermal expansion of floors would be significantly important for both reinforced concrete columns and floors. Depending on the stiffness and load capacity of the structural elements, collapse of reinforced concrete structures in fire could be initiated as a result of shear failure or bucking of beam due to large floor sagging, shear failure or buckling of columns, or even shear failure of the connections. In all these three failure modes, shear mechanism plays the major role and governs the performance of reinforced concrete structures in fire.
As mentioned earlier, drifts of columns due to thermal expansion of floor are very similar to the response of a column to an extreme lateral load such as an earthquake. This means buildings located in and designed for a low seismic risk area are even more vulnerable to thermal expansion than those in high seismic zones. This is mainly because reinforced concrete buildings designed for high risk of earthquake have relatively high shear and deformation capacity against lateral force and deformation. Therefore, studies on this subject would be extremely important for reinforced concrete buildings designed with low lateral loads such as earthquake. However, this would not entirely resolve the thermal expansion effects in buildings designed for high lateral force. In fact for such buildings, interaction of fire and earthquake, during the main shock and aftershocks, would be a major structural response, in which little knowledge and information is available. Thus, further studies are also needed to take into account the fire-earthquake interaction of the structures in the design or assessment process [14].

Normal-strength concrete High-strength concrete

Fig. 3. Spalling of concrete column after fire-resistance tests [12].

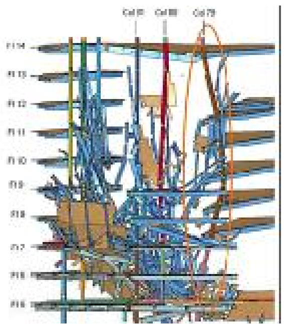

Fig. 4. Collapse simulation of WTC Building 7 [1].

3 STEEL STRUCTURES IN FIRE

Compared to reinforced concrete structures, steel framed buildings exposed to fire tend to perform poorly [15]. This is mainly because structural steel elements are relatively much thinner and have a higher thermal conductivity compared to concrete elements. Common failure modes of steel frames in fires are squashing, overall buckling, bending and lateral torsional buckling of columns, local buckling and bending failure of beams, and shear and local buckling failure of the connection elements [16]. Studies on behaviour of steel structures in fire show that end restraint and continuity of structural elements and membrane action of the floor slab would enhance performance of steel structures in fire [17, 18].

Axial restraint has a less profound influence on steel structures than on concrete structures. This is because the more rapid heating and the more ductile behaviour of steel structure can result in larger vertical deflections, floor sagging, which reduce the horizontal axial resistance force [15]. In other words, horizontal deformations as a result of thermal expansion of structural elements are relatively larger for reinforced concrete structures compared to steel-framed buildings. Therefore in steel structures, unlike reinforced concrete structures, most likely, floor sagging or deflection of beams is larger than column deformation or drift, which in fact coincides with the basic design philosophy of beam failure prior to column.

Recent study on the collapse of Word Trade Centre steel frame Building 7, has demonstrated that thermal expansion could be one of the major grounds for progressive collapse of steel buildings [1]. Fig. 4 illustrates progressive collapse simulation of Building 7, initiated by buckling of a column.

Results from an analytical study on behaviour of a steel structural system with perimeter moment resisting frame also indicate that floor thermal expansion can cause large out-of-plate displacement and inelastic stresses in the perimeter columns [19]. Studies also have been carried out on the effects of heating rate on the structural response. The results of these studies show that a slow heating rate could produce higher compressive forces in the connections of steel structures due to less thermal gradient and therefore less curvature to take out the thermal expansion of the beam [20]. In other words the heating rate has an important effect on the floor expansion; the slower the heating rate the higher floor thermal expansion is expected. This would convey that the decay or cooling down rate could also have significant effects on the thermal expansion of structural elements. Further studies are needed to investigate the effects of heating and cooling rates on performance of structures exposed to fire.

Currently, there are thermal transfer analytical tools available, such as SAFIR [21], for prediction of steel beam temperature during fire. However, available analytical tools for heat transfer analysis of concrete could not provide proper accuracy. For instance, the SAFIR program predicts higher temperatures for concrete, compared to the test data, which could be due to effects of the concrete moisture content property [22]. Further investigations are required to examine the problem and to develop proper analytical tools for heat transfer analysis of concrete slab and composite structures.

4 CONCLUSIONS

A literature review was carried out to explore a number of current studies on performance of structures in fire. The main considerations are primarily directed toward performance-based evaluation and design approaches. Among the research avenues recommended in this study, thermal expansion of structure was identified as one of the most important phenomena that requires a comprehensive research in order to understand the thermal expansion mechanism and its effects on the structural performance and to develop proper analytical and design approaches. There is currently a lack of design tools in buildings codes and standards for consideration of thermal expansion. For reinforced concrete structures there are very few models for material properties and shear failure mechanism at elevated temperature. Spalling mechanism of post-tensioned concrete structures requires further research. Studies are suggested on the effects of heating and cooling rates on the thermal stress and strain properties of structures. The cooling and heating rate would affect the magnitude of vertical and lateral deformations of structures. Effects of thermal properties and moisture content on spalling of concrete require further studies. The study on the collapse of Building WTC 7 showed the importance of a performance-based approach for the evaluation and design of structures in fire. Further studies are suggested on developing simple analytical approaches for modelling the response of 3D structural systems in fire. Studies are also recommended on developing thermal analytical approaches for reinforced concrete elements considering factors such as moisture content. Performance of structures exposed to different fire scenarios, including post-earthquake fire, requires assessment and research to develop realistic design fires and loading.

REFERENCES

[1] NIST, Final Report on the Collapse of World Trade Center Building 7, *National Institute of Standards and Technology*, www.nist.gov, November 2008.

[2] Beitel J., Iwankiw N, Analysis of Needs and Existing Capabilities for Full-Scale Fire resistance testing, *National Institute of Standards and Technology*, NIST GCR 02-843, 2002.

[3] Gross J. L., McAllister T. P., Structural Fire Response and Probable Collapse Sequence of the World Trade Center Towers, *National Institute of Standards and Technology,* NCSTAR 1-6, Federal Building and Fire Safety Investigation of the Word Trade Center Towers 2005

[4] Usmani A., A Very Simple Method for Assessing Tall Building Safety in Major Fires, *Proceedings of the Fifth International Conference on Structures in Fire*, May 2008.

[5] Sunder S., Report on the Collapse of World Trade Center Building 7, Opening Statement Press Briefing - August 21, 2008, *National Institute of Standards and Technology*, wtc.nist.gov, 2008

[6] Bailey C., Holistic behaviour of concrete buildings in fire, *Proceedings of the Institution of Civil Engineers. Structures and buildings*, vol. 152, Issue 3, pp. 199-212, 2002.

[7] Kodur V.K.R., Dwaikat M., Performace-based Fire Safety Design of Reinforced Concrete Beams, *Journal of Fire Protection Engineering*, Vol. 17, pp. 293-320, 2007

[8] Malhotra HL. Spalling of Concrete in Fires. Technical report. 118. *Construction Industry Research and Information Association*: London, 1984.

[9] Phan, L. T., Fire Performance of High-Strength Concrete: A Report of the State-of-the-Art, *National Institute of Standards and Technology*, NISTIR 5934, 1996

[10] Bostrom and Jansson, Results from Two Research Program on Spalling of Concrete, *Proceedings of the Fifth International Conference on Structures in Fire*, May 2008.

[11] Kodur V.K.R., McGrath R., Leroux P. and Latour J.C., Experimental Studies for Evaluating the Fire Endurance of High-Strength Concrete Columns, *National Research Council Canada*, No. 197, 2005.

[12] Kodur V.K.R., Fire Performance of High-Strength Concrete Structural Members, *National Research Council of Canada*, Construction Technology Update No. 31, 1999.

[13] Rowson J., Fire test exposes flaws in post-tensioned floor slabs, *New Civil Engineer*, *www.nce.co.uk*, 2008.

[14] Mousavi S., Bagchi A., Kodur V.K.R., Review of post-earthquake fire hazard to building structures. *Canadian Journal of Civil Engineering*, Vol.35, pp. 689–698, 2008.

[15] Buchanan A. H., Structural Design for Fire Safety, *John Wiley & Sons, 2001.*

[16] British Steel plc, Swinden Technology Centre, The Behaviour of Multi-Story Steel Framed Buildings in Fire, *British Steel plc, Swinden Technology Centre*, 1999.

[17] Nwosu D.I., Kodur V.K.R., Behaviour of Steel Frames Under Fire Conditions, *Canadian Journal of Civil Engineering*, 26, 156-167 (1999).

[18] Nwosu D.I., Kodur V.K.R., Steel Structures Exposed to Fire – A State-of-the-Art Report, *National Research Council Canada*, Report No. 749, 1997

[19] Varma, A.H., Agarwal A., Hongo S., Prasad K., Behaviour of Steel Building Structures With Perimeter MRFs Under Fire Loading Effects, *Proceedings of the Fifth International Conference on Structures in Fire*, May 2008.

[20] Selamet S., Garlock M. E. M., Behaviour of Steel Plate Connections Subjected to Various Fire Scenarios, *Proceedings of the Fifth International Conference on Structures in Fire*, May 2008.

[21] Franssen J. M., User's Manual For SAFIR 2007a Computer Program For Analysis of Structures Subjected to Fire, *University of Liege*, Belgium, 2007.

[22] Alfawakhiri F., Kodur V.K.R., Frater G., Temperature Field Modeling of the First Cardington Test, *National Research Council Canada*, NRCC-46898, 2004.

INTEGRITY OF FIRE RESISTANT CONSTRUCTION

- Developing A Methodology To Control Fire Induced Progressive Structural Collapse

Yong C Wang
University of Manchester, School of Mechanial, Aerospace and Civil Engineering, Manchester, UK

ABSTRACT

This paper is intended to initiate a discussion to develop a suitable framework within which design to control fire induced progressive structural collapse may be undertaken. There are two levels of integrity of fire resistant construction: prevention of fire spread (fire integrity) and control of progressive collapse (structural integrity). These two requirements have traditionally been considered in isolation with the formal being a purely fire but non-structural problem and the latter a purely structural problem. Using a few well-publicised recent examples of fire induced progressive structural collapse, this paper argues that while fire integrity should be achieved under "normal" fire design condition, when assessing structural integrity under exceptional fire loading, it may be necessary to assume some fire integrity failure and the simultaneous actions of fire and mechanical loading (structural response) should be considered. This may be likened to acceptance of local structural failure when assessing structural integrity in general. Modern structural fire engineering is seen by many to offer significant advantages (reduced construction cost, better understanding of structural behaviour leading to rational decision making on fire safety level) than the traditional prescriptive approach of fire resistant design. However, its inappropriate use could lead to increased risk of fire induced progressive collapse. Using tensile membrane action in floor slabs as an example, this paper suggests that the key element approach, similar to that in design for structural robustness, should be adopted.

1 INTRODUCTION

Under normal fire design condition, a building should have sufficient integrity so as to prevent fire spread through the building's fire resistant compartments. This is required to ensure that the risk to life safety and building damage is limited. Under exceptional fire exposure, the building structure should possess sufficient robustness so that the building does not suffer from progressive collapse. These requirements will be termed "fire integrity" and "structural robustness" respectively in this paper. Currently, design for "fire integrity" is poorly informed, with supporting information being mainly from standard fire resistance tests of building components. On the other hand, although there are some design guidelines on "structural robustness", they have not been developed with fire exposure in mind and may not be adequate for applications under exceptional fire condition. Furthermore, when these two aspects are considered, they are usually treated independently, with the fire engineer/architect responsible for "fire integrity" and the structural engineer responsible for "structural robustness". However, the recent high profile cases of fire induced progressive structural failure suggest that these two aspects are closely linked: fire integrity failure caused progressive structural collapse. In particular, multiple floor fires drastically increased the risk of progressive structural collapse. In order to establish that fire integrity failure and multiple floor fires should be considered as credible scenarios of exceptional fire loading, the next section will present a brief analysis of a few case studies.

2. A BRIEF ANALYSIS OF RECENT FIRE INDUCED PROGRESSIVE COLLAPSE

In the World Trade Center 1 and 2 buildings [1], airplane impact destroyed a number of floors and simultaneously ignited these floors. Furthermore, destruction of fire protection to the floor trusses by airplane impact caused the floor trusses to exceed their limiting temperatures in bending so that these floor trusses experienced very high deflections and developed catenary action. Simultaneous catenary action in these floor trusses meant that instead of them providing the edge structure with lateral restraint, the edge structure of WTC 1 & 2 buildings acted as compressive members with unrestrained lengths of a number of floor heights, with additional lateral forces acting on them. Progressive collapse of the buildings was inevitable.

In WTC 7 building [2], fire integrity of the building was also breached because the fire was present on a number of floors, Figure 1. In addition, the fire on each floor appeared to be travelling, reaching different intensities at different locations at different times. This resulted in fracture of the weak seated connection to column 79 (Figure 2), which led this column to become laterally unsupported at the floor level (Figure 3), which ultimately resulted in its bucking and progressive collapse of the building.

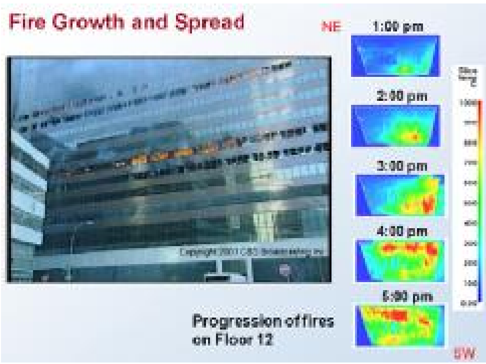

Figure 1: Multiple floor and travelling fire

Figure 3: Unsupported column 79

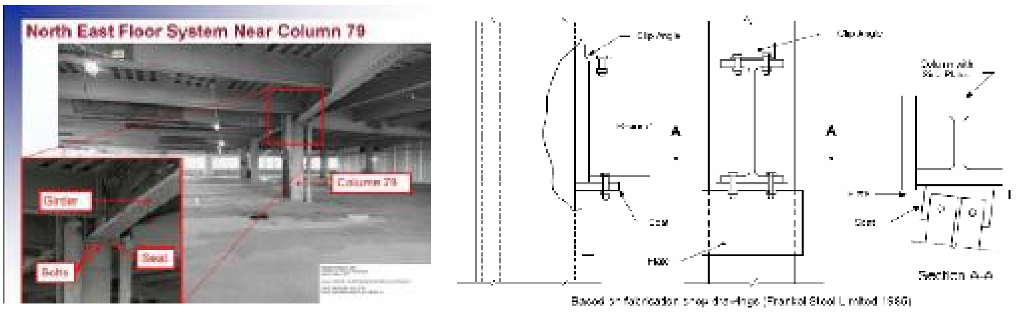

Figure 2: Seated connection to column 79 in WTC7 (FEMA 2008)

During the fire attack on the Madrid Winsor tower [3], poor fire stop between different fire compartments caused the fire to engulf a number of floors, which caused partial collapse on a number of floors, Figure 4. Fortunately, the strong and stiff core and floor slabs prevented total collapse of the structure.

These three cases of fire induced partial or complete structural collapse share one thing in common: the fire attack caused fire integrity failure and involved multiple floors. Whilst it would not be impossible for fires within one floor height to induce complete structural collapse, as will be postulated later, the risk of progressive structural collapse under multiple floor fires must be drastically higher than that under one floor fire. As has been demonstrated above, the exceptional fire loading scenario of fire integrity failure and multiple floor fire must be considered.

Fig 4: Madrid Windsor tower (Intermac 2005)

Multiple floor fires in the WTC buildings were caused by ignition on multiple floors (airplane impact on WTC1 and WTC2 and firebands from WTC1/WTC2 to WTC7), which by-passed the buildings' fire resistant compartmentation designed to prevent fire spread through floors. For some extremely important buildings, design for airplane impact may be a realistic scenario. If so, the probability of multiple floor fire must be very high. Other similar causes of multiple floor fires could include: explosion followed by fire and vehicle impact followed by fire.

In the Madrid Windsor tower, multiple floor fire was caused by poor compartmentation in the building. Although in general fire safety design, this cause may be eliminated through proper design and construction of the building's fire resistant compartmentation, it may be difficult to achieve because fire integrity is still rooted in the prescriptive framework of standard fire resistance testing and consideration of element performance. Although experiences so far may be used to indicate satisfactory performance of the current method of specifying fire integrity, as evidenced by infrequent report of fire integrity failure, this may have been purely good luck or underreporting as fire integrity failure has been observed in fire tests in buildings which have been constructed according to the prevailing specification and technology.

Other credible causes of multiple floor fires include fire spread through façade, either externally or internally in atrium construction, arson attack and fire following an earthquake.

3. OTHER POSSIBLE PROGRESSIVE COLLAPSE SCENARIOS

Under normal fire resistant design condition, it is assumed that the fire resistant compartmentation remains intact. Therefore, fire exposure is contained within the fire resistant compartment. Usually, a fire resistant compartment is within one storey of the building so the design assumption is that only the structure within the fire resistant compartment is exposed to fire. Furthermore, it is assumed that only one fire exposure is dealt with at a time, therefore, the accumulative effect of fire attack is not considered. But such an effect may lead to progressive collapse. For example, consider the 2-D skeletal structure shown in Figure 5, assuming each bay being a fire resistant compartment. Under normal fire design, the fire exposure will be in each of the bays and will be considered individually. Suppose fire is in bay 2. Further assume that the connection between the beam B2 and the column C2 is fractured due to axial force in the beam. It is possible that progressive collapse may occur following this event. But for the sake of argument, assume the structure is robust enough to limit the structural and fire damage to the connection only. Therefore, the buckling length of the column will not be changed because beam B1 will still be able to offer lateral support to the column. Now suppose fire design is now dealing with fire exposure in bay 1. The effect of fire exposure in bay 2 will now not be considered. Suppose the connection between beam B1 and column C2 is now fractured. The buckling length of column C2 will still not be changed because beam B2 is now providing lateral support to the column. Therefore, if fire in bay 1 and in bay 2 is considered separately, column C2 will be able to support the structure. However, if the fire is moving and travels from bay 1 to bay 2, or vice versa, then the connections on both sides of column C2 would be fractured and the column buckling length would be doubled, increasing the risk of progressive collapse. This appears to have contributed to progressive collapse of the WTC7 building.

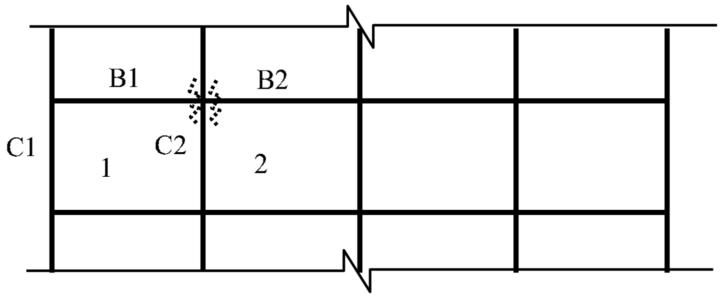

Figure 5: Illustrative example of loss of lateral support to columns

To summarise, fire integrity is concerned with prevention of fire spread. Design for fire integrity is necessary under "normal" fire scenario to limit the loss of fire damage. However, under exceptional fire attack, fire integrity failure may occur and this should be assumed when assessing structural integrity under exceptional fire exposure. Although it will not be possible to prescribe the number of multiple floor fires, the case of fire spread to adjacent fire resistant compartments should be considered. In addition, as illustrated above, it is possible for the supporting columns to become laterally unsupported over two floors even if fire exposure is contained within one floor height. Therefore, design for structural integrity under exceptional fire loading should consider the case of the vertical members being unsupported over two floor heights.

4. KEY ELEMENTS

A further potential source of progressive collapse is the continued push to extract the last possible source of reserve in capacity of the structure. Traditionally, fire resistant design has followed a rather elementary approach, in its treatment of the structure (based on structural elements, not the entire structure) as well as structural behaviour (according to the familiar small deflection theory, not large deflection behaviour). The result of this historical ignorance is that there is usually a substantial amount of reserve in fire resistance in the structure, which may become useful in controlling progressive collapse under exceptional fire conditions. Recently, refined methods have being developed to allow the reserve in structural capacity to be exploited, principally to reduce the need for fire protection. However, it is important that pushing the boundary in research is accompanied by appropriate caution and understanding in applications so that the risk of progressive structural collapse is not unduly increased.

Consider two recent developments in structural fire engineering: catenary action in beams and tensile membrane action in floor slabs. Tensile membrane action exploits the ultimate strength of a floor slab under very large deflections. One of the main assumptions is that the slab has to be vertically supported around all the edges. Under the normal design fire condition, it may be assumed that this key assumption is satisfied and that the benefit of tensile membrane action can be safely utilised. However, should an exceptional fire or other loading condition results in the loss of one of the edges of the slab, the slab would fold without being able to develop tensile membrane action and the applied load on the floor slab (designed according to tensile membrane action) could be much higher than the actual load carrying capacity of the slab, thereby greatly increasing the risk of progressive collapse. To a watchful engineer who is aware of this issue, the risk of progressive structural collapse may be reduced if the engineer takes appropriate actions. However, the commercial interest in utilising tensile membrane action has been such that it is now becoming routine application with decreasing level of understanding of the fundamental assumptions of structural behaviour. Contrast this with exploitation of catenary action. This load carrying mechanism is activated when an axially restrained beam undergoes very large deflections. If the connections between the beam and the surrounding structure are sufficiently strong, it is possible for the steel beam to survive virtually any fire attack without fire protection, which makes it possible to eliminate fire protection to steel beams [4]. However, since this load carrying mechanism relies on the close interaction between the restrained steel beam and other structural members, the beam cannot be considered in isolation (as can the floor slab when utilising tensile membrane action), therefore, utilising catneary action will force the potential user to thoroughly analyse the behaviour of the whole structure to ensure that the entire structure is stable. Furthermore, if this load carrying mechanism were disrupted under an extreme loading situation, it may be argued that damage would be local to the structure because the catenary action force (axial tension in the beam) would be relieved, thus reducing the load on the rest of the structure.

It is in the nature of researchers to push the boundary of understanding and quantification of structural behaviour and for practitioners to take advantage of any new found reserve in structural resistance. However, it is important that when exploiting advanced analysis methods, the designer develops an understanding of the potential of increased risk in progressive collapse. To mitigate the potential risk of progressive collapse, the key element or element removal approach may be adopted.

6. A POSSIBLE FRAMEWORK FOR ASSESSMENT OF PROGRESSIVE STRUCTURAL COLLAPSE UNDER EXCEPTIONAL FIRE LOADING

Whilst design for fire integrity is a well defined requirement, design for structural robustness is ill-defined due to the unknown nature of the initiating accidental event. Coupled with a lack of detailed research on structural robustness under exceptional fire condition, it is not possible at this stage to offer detailed recommendations for design. However, based on the discussions in the preceding sections of this paper, the following framework may be considered:

(1) Under exceptional fire loading, some fire integrity failure should be allowed. The design task then becomes how to prevent progressive collapse of the structure following the assumed fire integrity failure.
(2) It appears that the main cause of progressive structural collapse in fire is buckling of the columns as a result of loss of the lateral support to the columns in fire. Assuming fire integrity failure of the fire resistant compartments is immediately above or sideway on the same floor, the likely increase in the column buckling length is to make it unsupported over two storeys. In a braced multi-storey building of equal floor height, this would lead to doubling of the

column buckling length. For this type of construction under normal design fire, the current European standards (EN 1993-1-2 [5], EN 1994-1-2 [6]) recommend the column buckling length to be 0.5 times the floor height. Doubling this value would make the column buckling length the same as the floor height, which would be the column buckling length for ambient temperature design. Therefore, to enhance structural robustness under exceptional fire loading, one specific action is to use the same column buckling length for fire design as for ambient temperature design.

(3) Similar to normal consideration of structural robustness at ambient temperature, it is necessary to consider the scenario of elemental removal. This may have some impact on structures that have been fire engineered using tensile membrane action. Should an element removal lead to extensive structural failure, this element should be treated as a key element for fire resistance.

7. SUMMARY

The main objective of this paper is to initiate a discussion and debate on integrity of structures under fire exceptional attack. It has outlined the difference in considerations for fire integrity and structural integrity. Structural integrity failure (progress collapse) appears to be closely related to fire integrity failure (fire spread). It may not be possible to prevent fire integrity failure under exceptional fire loading. Therefore, it is recommended that when assessing progressive structural collapse under exceptional fire loading, some fire integrity failure immediate to the fire resistant compartment under design should be assumed. Design to achieve structural integrity should then aim to prevent progressive structural collapse based on the new fire exposure condition. It is further recommended that the key element approach for ambient temperature design be adopted so that structural elements that are critical to the viability of a particular critical load carrying mechanism (e.g. the edge members of a floor plate designed using tensile membrane action) are offered additional protection/strengthening or the consequence of its failure is clearly understood and explicitly considered.

REFERENCES

[1] Federal Emergency Management Authority (FEMA 2002), World Trade Center Building Performance Study, FEMA, USA.

[2] National Institute of Standards and Technology (NIST 2008), Federal Building and Fire Safety Investigation of the World Trade Center Disaster: Structural Response and Probable Collapse Sequence of World Trade Center Building 7, Volume 2, National Institute of Standards and Technology Report NIST NCSTAR 1-9.

[3] Instituto Tecnico De Materiales Y Construcciones (Intemac 2005), Fire in the Windor building, Madrid: Survey of the fire resistance and residual bearing capacity of the structure after the fire, Intemac

[4] Yin, Y.Z. and Wang, Y.C. (2004), "A numerical study of large deflection behaviour of restrained steel beams at elevated temperatures", Journal of Constructional Steel Research, Vol. 60, No. 7, pp. 1029-1047

[5] Committee of European Standardisation (CEN 2005a), Eurocode 3: Design of steel structures, Part 1-2: General rules – structural fire design, BS EN 1993-1-2, British Standards Institution

[6] Committee of European Standardisation (CEN 2005b), Eurocode 4: Design of composite steel and concrete structures, Part 1-2: General rules – structural fire design, BS EN 1994-1-2, British Standards Institution

SUPER ELEMENT IN STRUCTURAL ANALYSIS

Yuan Weifeng, Tan Kang Hai
School of Civil & Environmental Engineering, Nanyang Technological University, Singapore 639798

INTRODUCTION

The computing cost in FEM analysis is dependant on the number of degrees of freedom (DOF) in the model under investigation. To increase computational efficiency, one direct way is to reduce the number of elements. However, the FEM theory indicates that fewer elements will cause poorer accuracy in general cases. To achieve a better balance between accuracy and processing time, several special techniques have been developed without altering the accuracy of numerical findings, for instances, the spectral finite element method [1] and the transfer matrix method [2]. Alternatively, super element method has been widely applied in the FEM analyses for various problems [3, 4, 5]. Briefly, the basic concept of super element method is to treat the structural members as a continuous body, and then discretize this continuous body into super elements using traditional FEM techniques [6, 7]. In this way, each super element may consist of different types of members which may have various shapes, material properties and boundary conditions. In this paper, the procedure of constructing super elements is introduced based on numerical examples. To implement the proposed approach, an entire structure has to be divided into several zones according to the requirement of numerical investigation and the expected behavior of the structure. Among all the zones defined by the user based on his judgment, some zones consist of linear members and the others have nonlinear members. The advantage of the proposed method is that all the linear zones can be grouped into one super element, regardless whether they are connected or not. The nodes of the super element include i) all the boundary nodes between linear and nonlinear zones and ii) an additional node which only has one DOF, if there are external loads acting on the members within the linear zones. Thus, the total number of DOF of the original FEM model can be reduced significantly. It is noteworthy that the same approach can also be applied to linear analyses although the saving may not be as remarkable as a non-linear analysis.

1 DEFINITION OF SUPER ELEMENT

1.1 Basic Concept

To illustrate the approach, recourse is made to a frame example as shown in Figure 1. The frame is evenly divided into twenty two-node three-dimensional beam elements, and three forces are applied at nodes 3, 9 and 21, respectively. It is assumed that in such a structure, greater attention is needed for key elements between node 6 and node 21. The zone comprising the key elements is denoted as a non-linear zone. In this case, all the elements between node 1 and node 11 can be merged into one super element, if only linear analysis is required for these elements. This is also the linear zone.

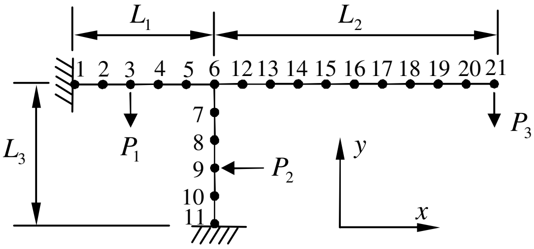

Figure 1. A two-dimensional frame subjected to external forces

Consider the linear zone shown in Figure 2, with the key elements including the force applied on them removed from the original model. To construct a super element, its nodes must be determined at the beginning. For the FEM model in Figure 1, node 6 is the only joint shared by the nonlinear and linear zones. Thus, the super element under construction will have only two nodes, viz. node 6 which has six DOFs and an additional node, which is in linear zone. Without loss of generality, node 8 is selected to be the second node of the super element.

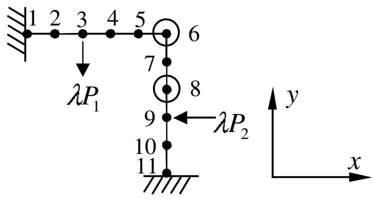

Figure 2. The linear zone of the two-dimensional frame under real forces

To obtain the stiffness matrix of the super element, a series of linear analyses has to be conducted based on the configuration shown in Figure 2:
Firstly, forces λP_1 and λP_2, where λ is an arbitrary nonzero factor are applied to the frame and the associated deformations at node 8 and node 6 are calculated. Denoted by ${}^0\boldsymbol{U}$, where the superscript indicates the load case number, the corresponding deformation vector induced by the combination of all scaled forces applied on the linear zones (λP_1 and λP_2 in this example) is expressed by ${}^0\boldsymbol{U} = ({}^0u_{8-x}, {}^0u_{6-x}, {}^0u_{6-y}, {}^0u_{6-z}, {}^0\theta_{6-x}, {}^0\theta_{6-y}, {}^0\theta_{6-z})^T$, where the terms u and θ represent the nodal displacements and rotations, respectively. The Arabic number in the subscript denotes the node number, while the Latin letters indicate the respective coordinate axis. It should be mentioned that all the six components of the deformation at node 6 are stored in ${}^0\boldsymbol{U}$ but only one component of the deformation of node 8 needs to be considered. In fact, among the six components of the deformation of node 8, any nonzero component can be selected to form ${}^0\boldsymbol{U}$.

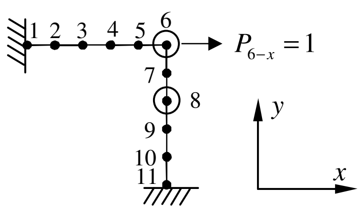

Figure 3. The linear zone of the two-dimensional frame under virtual force scenario

Secondly, as shown in Figure 3, the forces P_1 and P_2 are removed and a unit load P_{6-x} is applied to node 6 at the x direction. Similar to the first step, the deformations at node 8 and 6 are calculated and stored in ${}^1\boldsymbol{U} = ({}^1u_{8-x}, {}^1u_{6-x}, {}^1u_{6-y}, {}^1u_{6-z}, {}^1\theta_{6-x}, {}^1\theta_{6-y}, {}^1\theta_{6-z})^T$.

Thirdly, repeat the second step to generate five more load cases, viz. two unit loads (along the y and z-axis) and three unit moments (about x, y and z-axis) are applied to node 6 in sequence. The corresponding deformation vectors are stored as ${}^2\boldsymbol{U}$, ${}^3\boldsymbol{U}$, ${}^4\boldsymbol{U}$, ${}^5\boldsymbol{U}$ and ${}^6\boldsymbol{U}$. It should be mentioned that the global stiffness matrix of the linear zone shown in Figure 2 and 3 can be factorized during the calculation. Hence, ${}^1\boldsymbol{U} \sim {}^6\boldsymbol{U}$ can be obtained without additional effort compared with the solution procedure of ${}^0\boldsymbol{U}$. Based on the characteristic of linear elasticity, the above three steps can be described by one equation given by:

$$\boldsymbol{K}\boldsymbol{\psi} = \begin{pmatrix} 1 & \boldsymbol{0} \\ \boldsymbol{0} & \boldsymbol{I}_{6\times6} \end{pmatrix}_{7\times7} = \boldsymbol{I}_{7\times7} \tag{1}$$

where $\boldsymbol{\psi} = ({}^0\boldsymbol{U}, {}^1\boldsymbol{U}, {}^2\boldsymbol{U}, {}^3\boldsymbol{U}, {}^4\boldsymbol{U}, {}^5\boldsymbol{U}, {}^6\boldsymbol{U})$ and $\boldsymbol{K}$ is an unknown matrix.

It should be mentioned that in Eq. (1), the load case of the combination of λP_1 and λP_2 is represented by a unit virtual force "1" acting at node 8 in the x direction.

In the end, the inverse matrix of $\boldsymbol{\psi}$ is calculated. Based on Eq. (2), one obtains $\boldsymbol{K} = \boldsymbol{\psi}^{-1}$ where $\boldsymbol{K}$ performs as the stiffness matrix of the super element. For this example, the super element has seven DOFs, including six DOFs at node 6 and one DOF at node 8.

1.2 General Approach

Special attention must be paid to the case that the remaining structure is unstable after the part under investigation is removed from the original structure. For instance in Figure 4 (a), an elastic block is supported at points A and B by columns 1 and 2, respectively. In FEM modeling, the block may be meshed into many elements. However, to conduct an efficient analysis, all the elements on the block can be merged into just one super element. According to the present approach, points A and B must be selected to be the nodes of the super element. Moreover, another point, assuming to be point C, is also selected. To calculate the stiffness matrix of the super element, the proposed approach requires that the two columns must be removed from the original model. But the problem arising in this procedure is that the block above the two columns becomes unstable since it is hanging in the air without any physical support. Based on such a configuration, the deformation vectors of nodes A, B and C cannot be obtained.

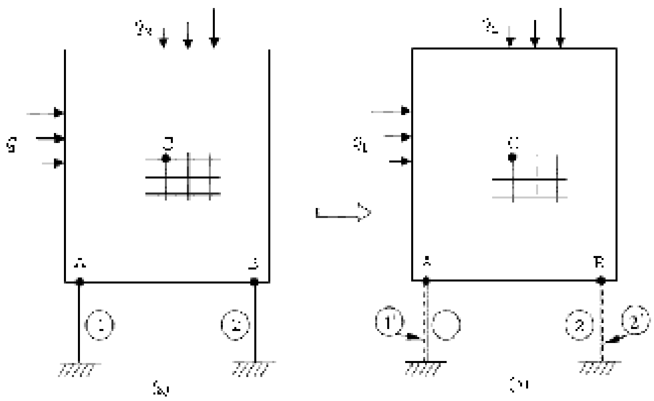

Figure 4. Calculate the stiffness matrix of super element using weak member method

To overcome the problem, a so-called “weak member method” is proposed in this paper. As illustrated in Figure 4 (b), two columns, viz. $1'$ and $2'$ are added to the original structure given in Figure 4 (a). The dimensions and locations of the old and new columns overlap each other, but columns $1'$ and $2'$ are much weaker than original columns 1 and 2. Theoretically, the numerical result based on (b) will not differ much from the one based on (a). Therefore, structure (b) can be used to replace structure (a) in ensuing analyses without affecting the accuracy of findings. Obviously, for structure (b), the remaining structure is still stable even if columns 1 and 2 are removed. Thus, based on structure (b), the stiffness matrix of super element can be carried out following the four steps described in Section 1.1.

2 NUMERICAL VALIDATION

2.1 Linear Analysis

Once the super element is constructed, the global stiffness matrix can be assembled using traditional approach. Meanwhile, the original frame given in Figure 1 is replaced by an equivalent structure shown in Figure 5. Please note that a fictitious force is applied at node 8. Its value is set to $1/\lambda$ since the actual forces P_1 and P_2 are scaled up to λP_1 and λP_2, respectively. In a nonlinear analysis, this fictitious force and P_3 are applied to the structure proportionally.

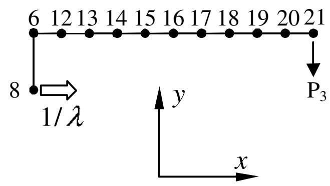

Figure 5. A FEM frame model consists of beam and super elements

To verify the correctness of the proposed approach, linear analyses are first conducted for the original frame using normal and super element approaches. In the simulation in Figure 1, it is defined that $L_1 = L_2/2 = L_3 = 0.5$. The dimension of the cross-section of each beam is set to be 0.05×0.05. The material properties of both super and normal elements are the same. Young’s modulus is set to 1×10^6 and Poisson’s ratio is set to 0.3. The loads applied to the original frame are $P_1 = P_2 = 10$ and $P_3 = 0.1$. During the calculation, the factor λ is set to 10.

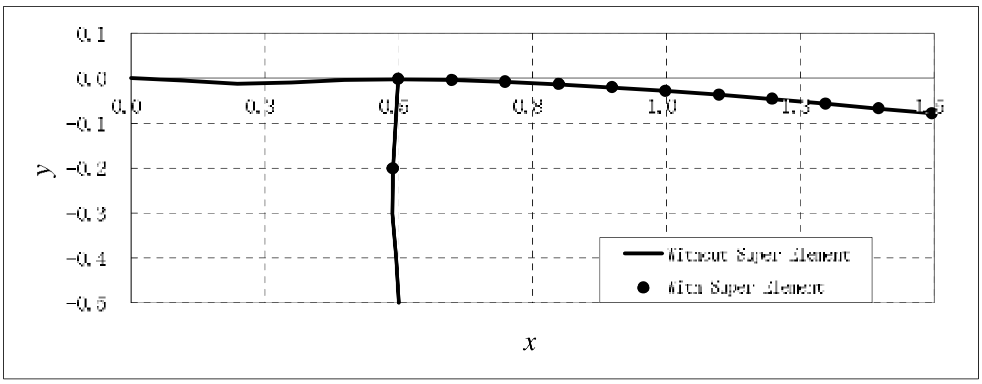

Figure 6. Comparison between the deformations obtained by FEM and super element method

The comparison between normal FEM and the proposed super element approach is depicted in Figure 6. In the figure, the deformations of the structure obtained by normal and the present FEM methods are compared. Obviously, with or without super element, the two results are almost the same.

2.2 Nonlinear Analysis

It is now assumed that nonlinear analysis is required for the frame shown in Figure 1. The geometry and the material properties are identical as the problem in Section 2.1. However, the forces at node 3 and node 9 are all zero, viz. $P_1 = P_2 = 0$. Meanwhile, P_3, the force at node 21 is replaced by a bending moment about z-axis. In this situation, the nonlinear response of the frame can be calculated using the model given in Figure 7. One finds that the fictitious force applied at node 8 is set to zero.

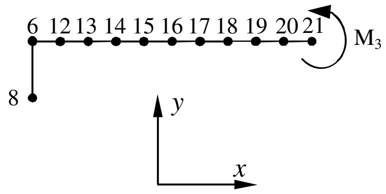

Figure 7. A FEM frame model with super element under bending moment

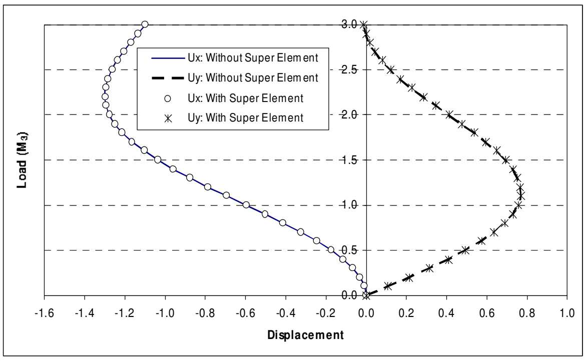

Figure 8. The load-displacement curves obtained by FEM and super element method

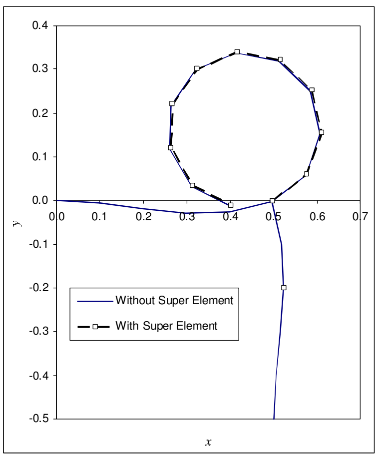

Figure 9. The shapes of the deformed frame obtained by FEM and super element method

Using load-control algorithm, a full nonlinear analysis is conducted for the model for 30 steps. In the simulation, the load increment in each step is set to 0.1. As a comparison, the model shown in Figure 7 is analyzed by super element method. The load-displacement relationships at node 21 are depicted in Figure 8. From the figure, one finds that the results obtained by super element method are very close to traditional FEM results. However, as shown in Figure 9, slight differences between the two kinds of results can be observed. This is caused by the assumption of linearity for super element.

3 CONCLUSION

This manuscript presents a method to construct super element. The advantage of the present method is that, with weak element formulation, different parts which may not be connected in a structure can be merged into one linear element to reduce the number of DOFs. Numerical examples show that this method is easy to be implemented and it has great potential in the simulation of large complex structures.

In traditional FEM, the global stiffness matrix is generally symmetric. However, it should be mentioned that this characteristic of the system matrix is damaged in the present method since the stiffness matrix of the super element is non-symmetric. On the other hand, although non-symmetric system matrix may cause additional requirements for CPU time, the overall calculation is efficient because the total number of DOFs is reduced significantly. Moreover, some techniques, such as iteration algorithm can be used to minimize the loss induced by non-symmetric matrix.

REFERENCES

[1] Finnveden S, Exact Spectral Finite Element Analysis of Stationary Vibrations in Rail Way Car Structure, *Acta Acustica*, (1994) 2: 461-482.

[2] Lin YK, Donaldson BK, A Brief Survey of Transfer Matrix Techniques with Special Reference of Aircraft Panels, *Journal of Sound and Vibration*, (1969) 10: 103-143.

[3] Ju F, Choo YS, Super Element Approach to Cable Passing Through Multiple Pulleys, *International Journal of Solids and Structures*, (2005) 42: 3533-3547.

[4] Jiang J, Olson MD, Nonlinear Analysis of Orthogonally Stiffened Cylindrical Shells by A Super Element Approach, *Finite Elements in Analysis and Design*, (1994), 18: 99-110.

[5] Lukasiewics SA, Geometrical Super-Elements for Elasto-Plastic Shells with Large Deformation, *Finite Elements in Analysis and Design*, (1987) 3: 199-211.

[6] Huang Y, Ma KJ, Chen B, The Study of Dynamic Behavior for Multi-Storied Vierendeel Sandwich Plate-Column Structure, *Journal of Building Structures*, (2000) 3: 23-29

[7] Cao ZY, Super Element Method for Complex Structure Analysis, *Mechanics and Practice*, (1992) 14 (4): 10-14.